https://ntrs.nasa.gov/search.jsp?R=19670013943 2018-07-23T02:42:23+00:00Z

First Order Effects of Production on the Continuum Theory of Spherical Electrostatic Probes

by

Ira M. Cohen & S. Schweitzer

Towne School of Civil and Mechanical Engineering
and the
Institute for Direct Energy Conversion

University of Pennsylvania
Philadelphia, Pennsylvania

INDEC - 47

February 1967

N67-23272
(ACCESSION NUMBER)
44
(PAGES)
CR 83545
(NASA CR OR TMX OR AD NUMBER)
(THRU)
1
(CODE)
25
(CATEGORY)
FACILITY FORM 602

First Order Effects of Production on the Continuum Theory of Spherical Electrostatic Probes

by

Ira M. Cohen* & S. Schweitzer**

University of Pennsylvania

February 1967

N67-23212

* Assistant Professor of Mechanical Engineering, Towne School of Civil and Mechanical Engineering, Member AIAA.

** Assistant Professor of Mechanical Engineering, Towne School and Institute for Direct Energy Conversion, Member AIAA.

This work has been supported partially by the Towne School of Civil and Mechanical Engineering and partially by NASA Grant NSG-316.

Abstract

The analysis of spherical Langmuir probes which are immersed in an infinite, homogeneous, slightly ionized, collision-dominated plasma is given to first order in the smallness of a parameter characterizing the effects of ionization and recombination. The treatment is given as a double limit: mean free path << sheath thickness << probe radius (as in the antecedent works) and the weakness of production effects. The first limit separates the system of equations into two regions: a quasi-neutral region and a thin collision-dominated space charge sheath. The second limit of weak production further separates the quasi-neutral region into two subsidiary regions: a main region in which the production effect is a regular perturbation and a distant region where gradients are weak and the small production is of the same order as diffusion. The governing diffusion equations are solved to lowest order in $\rho_p = r_p/\lambda_D$ and to first order in the smallness of the production parameter. Current-voltage characteristics are computed from integrals of the solutions and emphasis is placed on their interpretation with respect to measurements. An experimental procedure is outlined which yields in turn $D_- N_o$, T_-/T_+, D_+/D_-, and the production parameter, where D is diffusion coefficient, T is temperature and N_o is the undisturbed ion or electron density. The first order effects of ionization and recombination are also discussed. It is found for $T_-/T_+ = 1$ that, at negative probe potentials, the normalized ion current to the probe is increased and the electron current decreased. At positive probe potentials, on the other hand, the ion current to the probe is decreased and the electron current increased by the effect of production. For $T_-/T_+ > 1$, the same effect is observed for negative probe potentials but, for positive probe potentials, no such general statement can be made. For a ten percent change in the production parameter, for example, we find that the relative change in the currents is at most slightly more than ten percent (for fixed probe potential).

A. Introduction

In many cases of ionized gas flows, the gas is not so weakly ionized that only charged-neutral collisions occur. For ionization fractions greater than about 10^{-4}, the effects of charge-charge collisions must be taken into account.[1,2] There are three effects of charge-charge collisions that change the formulation and consequently the results of the earlier asymptotic theories of electrostatic probes.[3,4,5] These are (1) the dependence of diffusion coefficients on charged particle densities and therefore position; (2) volume recombination of charged particles; and (3) volume production of charged particles. Su and Sonin[6] have allowed for charge-charge collisions in their electrostatic probe theory in which they have used the lowest order diffusion coefficients (in the Chapman-Enskog sense[7]) which depend only on the neutral distribution and therefore are constant (since the neutrals are assumed to be uniformly distributed). They have shown that to lowest order in an expansion based on the limit $r_p/\lambda_D \to \infty$ (r_p is probe radius, λ_D is Debye length), a transformation of the electrostatic potential reduces the new problem to one that has been solved.[3,4] In general, however, the diffusion coefficients are not constant and such a reduction is not possible. Whitman and Yeh[8] treat spherical probes in a seeded inert gas plasma with ionization due to electron impact on seed neutrals and recombination due to three body electron impact (2 electrons + ion). An external electric field is maintained so electrons can accelerate to ionization potential. Moreover, the space charge sheath is assumed to be collisionless and the disturbed diffusion dominated region around the probe is assumed to be so thin that curvature effects are neglected. The latter is possible only if production and recombination effects are significant, implying a significant number of three body collisions. This is certainly not consistent with the assumption of constant diffusion coefficients. Also the matching of a collision-dominated diffusion region with a collisionless sheath as done by Davydov and Zmanovskaja[9] is impossible in principle as explained in Sect. A of Ref. 4.

In the present paper we shall assume that the gas is still weakly ionized so that charged-neutral collisions predominate. Therefore production and recombination will be small effects and we shall present a continuum theory to first order in the smallness of production. However, to keep the theory as simple as possible we shall neglect the correction to the diffusion coefficients (which is of the same order of smallness as the production terms which we retain). This is justified by the fact that since both effects are small perturbations of the main problem[3,4] their separate contributions are additive*. Thus it is necessary only to treat them one at a time: production and recombination here; part of the effect on diffusion coefficients by Su and Sonin.[6]

We perform a double limit process on the governing diffusion equations and Poisson's equation. The limit $\rho_p \to \infty$ (where ρ_p is the ratio of probe radius to Debye length based on undisturbed properties) splits the equations into two regions: a quasi-neutral region and a thin space charge sheath near the probe surface. The limit of weak ionization and recombination splits the quasineutral region into a main quasineutral region, where the effects of production are a regular perturbation, and a distant quasineutral region, where gradients are so weak that the effects of production must be accounted for in the dominant order. The solutions in all three regions are obtained to first order in the production parameter and to dominant order in the largeness of ρ_p. Asymptotic matchings of the solutions are performed in the overlap domains where solutions in adjoining regions are both valid. We find, as expected, that production is unimportant in the sheath because density levels are very low there. Thus the sheath equations are identical to those solved in Ref. 4.

---

* The equations governing the first order perturbations are linear. Thus the effects of production and the effects of three body collisions on the diffusion coefficients appear as separate inhomogeneous terms. The solutions for each of these effects may be obtained separately and are additive.

From our solutions we obtain current-voltage characteristics for various values of the production parameter and then outline a sequence of measurements to apply the theory to experimental situations. We show how one would measure $D_- N_o$, T_-/T_+, D_+/D_-, and the production parameter from experimentally obtained current-voltage characteristics. (Here, D is diffusion coefficient, T is temperature, N_o is undisturbed plasma density.)

We find for $T_-/T_+ = 1$ that, at negative probe potentials, the normalized ion current to the probe is increased and the electron current decreased. At positive probe potentials, on the other hand, the ion current to the probe is decreased and the electron current is increased by the effect of production. For $T_-/T_+ > 1$, the same effect is observed for negative probe potentials, but no such general statement can be made for positive probe potentials. For a ten percent change in the production parameter, for example, we find that the relative change in the currents is at most slightly more than ten percent (for fixed probe potential). The effects of temperature ratio and ratio of probe radius to Debye length are the same as in Ref. 4.

B. Statement of the Problem

We start with the equations governing the diffusion of charged particles in a force field--conservation of mass for ions and electrons. These are

$$\nabla \cdot \underset{\sim}{\Gamma}_+ \equiv \nabla \cdot [-D_+ \nabla N_+ - \mu_+ N_+ \nabla \varphi] = \nu_p N_- N_n - \nu_r N_+ N_- N_n \tag{1}$$

$$\nabla \cdot \underset{\sim}{\Gamma}_- \equiv \nabla \cdot [-D_- \nabla N_- + \mu_- N_- \nabla \varphi] = \nu_p N_- N_n - \nu_r N_+ N_- N_n \tag{2}$$

where $D_\pm/\mu_\pm = kT_\pm/e$. We have also Poisson's Eq.

$$\nabla^2 \varphi = -4\pi e [N_+ - N_-] \tag{3}$$

for the self-consistent electric field. Here $\underset{\sim}{\Gamma}_\pm$ are the particle flux vectors of ions and electrons, D is the diffusion coefficient, μ is the mobility coefficient, T is the temperature, $N_\pm$ is the ion or electron number density, N_n is the neutral density, φ is the electrostatic potential, k is Boltzmann's constant, e is the charge on an electron, ν_p and ν_r are production and recombination coefficients (note the different units) and subscripts + and - refer to ions and electrons, respectively. We shall assume that ν_p, ν_r, N_n, D and μ are all constant. The validity of the model is discussed in references 4 and 10. We have assumed production by electron-neutral impact (without postulating an external electric field as in Ref. 8 to accelerate the electrons) and recombination by three body collisions. Any other mechanisms the reader may prefer may be substituted for these; the procedure that follows will not be affected.
The boundary conditions for Eqs. (1) through (3) are:

$$\text{on the probe surface:} \quad N_+ = N_- = 0, \ \varphi = \varphi_p \tag{4}$$

$$\text{at infinity:} \quad N_+ = N_- = N_o, \ \varphi = 0$$

The zero density condition is a consequence of the assumption that the probe absorbs all charged particles incident upon it and of the smallness of the mean free path.* In the $r_p/\lambda_D \to \infty$ limit, however, the charged-neutral mean free path may be of the same order as the Debye length based on undisturbed properties (Ref. 4, Section A).

Since the plasma is uniform at infinity ν_p and ν_r must be related so that the right hand side of Eqs. (1) and (2) is zero when the left hand side is zero. Therefore,

$$\nu_p = N_o \nu_r \tag{5}$$

We normalize the equations via

$$\zeta = r_p/r,\ n_\pm = N_\pm/N_o,\ \psi = e\varphi/kT_-,\ \tau = T_-/T_+,\ \delta = D_+/D_-,$$

$$\alpha = \nu_r N_n N_o r_p^2/D_+,\ \rho_p = r_p/\lambda_D,\ \lambda_D = [kT_-/(4\pi N_o e^2)]^{1/2}, \tag{6}$$

$$\psi_p = e\varphi_p/kT_-,\ \text{and}\ (\ )' = \frac{d}{d\zeta}$$

This yields

$$\zeta^4 (n_+' + \tau n_+ \psi')' = -\alpha n_-(1 - n_+) \tag{7}$$

$$\zeta^4 (n_-' - n_- \psi')' = -\delta\alpha n_-(1 - n_+) \tag{8}$$

$$\frac{\zeta^4}{\rho_p^2} \psi'' = n_- - n_+ \tag{9}$$

$$\zeta = 1:\ n_+ = n_- = 0,\ \psi = \psi_p \tag{10}$$

$$\zeta = 0:\ n_+ = n_- = 1,\ \psi = 0 \tag{11}$$

We shall consider the limits $\rho_p \to \infty$ and weak production ($\alpha \to 0$) on Eqs. (7-11).

* This boundary condition has been derived rigorously by Burke and Lam, AIAA Paper 67-100, Section III.C.1.

C. Asymptotic Solution: $\rho_p \to \infty$ and $\alpha \to 0$

The $\rho_p \to \infty$ limit splits Eqs. (7-11) into two regions: a quasi-neutral region ($n_\pm$, $d/d\zeta$ finite) and a space charge sheath ($n_\pm$ small, $d/d\zeta$ large). We shall treat these in turn.

1. Quasi-Neutral Region

Away from the probe surface where $n_\pm$ and derivatives are finite, Eq. (9) gives

$$n_+ = n_- + O(\rho_p^{-2}) \tag{12}$$

Neglecting the higher order correction and denoting by n the common value of the density, we may eliminate ψ from Eqs. (7) and (8) yielding for n

$$\zeta^4 n'' = -A n (1-n) \qquad (n(0) = 1) \tag{13}$$

where $A = \frac{(1+\delta\tau)}{(1+\tau)} \alpha < \alpha$ since $\delta < 1$ when electrons carry the negative charge. Thus, $\alpha \to 0$ implies $A \to 0$. For $A \to 0$, there are two distinct regions in Eq. (13): (1) $\zeta > O(A^{1/2})$ where the right-hand side is a small perturbation on the left-hand side, and (2) $\zeta \leq O(A^{1/2})$ when both sides of Eq. (13) are the same order. We call these regions the main region [$\zeta > O(A^{1/2})$] and the distant region [$\zeta \leq O(A^{1/2})$] respectively.

Once Eq. (13) has been solved for n, we obtain the equation for ψ by subtracting Eq. (8) from Eq. (7), yielding to $O(\rho_p^{-2})$,

$$(n\psi')' = -\frac{B n (1-n)}{\zeta^4} \qquad (\psi(0) = 0) \tag{14}$$

where $B = \frac{(1-\delta)}{(1+\tau)} \alpha = \frac{(1-\delta)}{(1+\delta\tau)} A = O(\alpha)$.

(a) Main Region $\zeta > O(A^{1/2})$

To lowest order in the main region, A is taken to be zero, giving

$$n = c_1 - c_2 \zeta + O(A) \tag{15}$$

where c_1 is found by matching with the distant region and c_2 is found by matching

with the space charge sheath. To next order in the main region,

$$n = c_1 - c_2\zeta - A\left[\frac{c_1(1-c_1)}{6\zeta^2} + \frac{c_1 c_2}{2\zeta} - \frac{c_2(1-c_1)}{2\zeta} + c_2^2 \ln\zeta\right] + O(A^2) \quad (16)$$

From Eq. (14) for ψ, we have to lowest order

$$\psi' = \frac{c_3}{c_1 - c_2\zeta}, \qquad \psi = -\frac{c_3}{c_2}\ln(c_1 - c_2\zeta) + O(A) \quad (17)$$

and, to next order,

$$\psi' = \frac{c_3}{c_1 - c_2\zeta}\left\{1 + \frac{A}{c_1 - c_2\zeta}\left[\frac{c_1(1-c_1)}{6\zeta^2} + \frac{c_1 c_2 - c_2(1-c_1)}{2\zeta} + c_2^2 \ln\zeta\right]\right\}$$

$$- \frac{B}{c_1 - c_2\zeta}\left[\frac{-c_1(1-c_1)}{3\zeta^3} - \frac{c_1 c_2 - c_2(1-c_1)}{2\zeta^2} + \frac{c_2^2}{\zeta}\right] + O(A^2) \quad (18)$$

We must consider the distant region to determine c_1 and obtain a complete quasi-neutral solution. The constant of integration c_3 is obtained by matching with the space charge sheath.

(b) <u>Distant Region $\zeta \leq O(A^{1/2})$</u>

For $\zeta = O(A^{1/2})$, both sides of Eq. (13) are of the same order. However, because of the boundary condition, n is near 1 for <u>all</u> small ζ (in particular $\zeta \leq O(A^{1/2})$). In the distant region, therefore,

$$n = 1 - n_1, \quad n_1 \ll 1, \quad n_1(0) = 0. \quad (19)$$

n_1 satisfies

$$\zeta^4 n_1'' - A n_1 = O(n_1^2) \approx 0 \quad (20)$$

$$n_1(0) = 0$$

which has the solution: $n_1 = \bar{c}_2 \zeta e^{-\sqrt{A}/\zeta} + O(\zeta^2 e^{-2\sqrt{A}/\zeta})$.

Thus

$$n = 1 - \bar{c}_2 \zeta e^{-\sqrt{A}/\zeta} + O(\zeta^2 e^{-2\sqrt{A}/\zeta}) \tag{21}$$

Matching in the overlap domain $[O(A^{1/2}) < \zeta < O(1)]$ with Eq. (15) gives

$$c_1 = 1, \quad \bar{c}_2 = c_2. \tag{22}$$

The corresponding potential gradient is

$$\psi' = \frac{-(B/A)\, c_2\, e^{-\sqrt{A}/\zeta}\,[\,1 + A^{1/2}/\zeta\,] + (Bc_2^2/2\sqrt{A})\, e^{-2\sqrt{A}/\zeta} + \bar{c}_3}{1 - c_2 \zeta e^{-\sqrt{A}/\zeta}} + O(\zeta^2 e^{-2\sqrt{A}/\zeta}) \tag{23}$$

where $\bar{c}_3$ is obtained by matching with Eq. (17) in the overlap domain. We find $\bar{c}_3 = c_3 + Bc_2/A$. We could go to next order in the distant region but this is not necessary to get the first order corrections to the probe characteristics for small α.

Note that if $c_2 > 1$, which is the case, $n \to 0$ and $\psi' \to \infty$ before the probe wall ($\zeta < 1$). Thus there is a singular point given by the zero of n:

$$\zeta_s = \frac{1}{c_2} - A\left(\frac{c_2}{2} - c_2 \ln c_2\right) + O(A^2) \tag{24}$$

in the neighborhood of which the quasi-neutral solution breaks down. It is clear that near the singular point n is small and derivatives are large. The treatment of the equations in the neighborhood of the singular point follows.

2. Space Charge Sheath

In the space charge sheath (the neighborhood of the singular point), the variables n_+, n_-, and ζ must be scaled by appropriate powers of ρ_p to render the new variables finite. Either by reference to the antecedent works[4,5] or to the "Principle of Maximal Balance"[11], we find the appropriate scalings are:

$$\bar{n}_\pm = \rho_p^{2/3}\, n_\pm$$
$$x = \rho_p^{2/3}\, \zeta_s^{-2}\, (\zeta - \zeta_s). \tag{25}$$

The flux equations may be integrated once and, in the scaled variables, are to lowest order in ρ_p,

$$\frac{d\bar{n}_+}{dx} + \bar{n}_+ E = -\bar{J}_+ + O(\rho_p^{-2/3})$$

$$\frac{d\bar{n}_-}{dx} - \bar{n}_- E = -\bar{J}_- + O(\rho_p^{-2/3}) \tag{26}$$

$$\frac{dE}{dx} = \bar{n}_+ - \bar{n}_- + O(\rho_p^{-2/3})$$

with the boundary conditions:

at $x = x_w = -\rho_p^{2/3} \zeta_s^{-2} (1 - \zeta_s) : \bar{n}_+ = \bar{n}_- = 0, \ \psi = \psi_p$

as $x \to -\infty$: $\bar{n}_+$, $\bar{n}_-$, E match with quasi-neutral solution where $E \equiv d\psi/dx$ and the constants of integration $\bar{J}_+$, $\bar{J}_-$ are related to the particle fluxes to the probe. These equations are the usual collision-dominated sheath equations of References 4, 5, 10, and 12. Following the usual procedure, we eliminate $\bar{n}_+$ and $\bar{n}_-$ in favor of E, integrate the resulting third order equation once, set the constant of integration to zero (consistent with the previous works) and apply the finite transformation:

$$E(x) = (\bar{J}_+ + \tau \bar{J}_-)^{1/3} F(t)$$
$$t = -(\bar{J}_+ + \tau \bar{J}_-)^{1/3} x. \tag{27}$$

The result is

$$F'' = (\tau - 1) FF' + \frac{\tau}{2} F^3 + tF + \lambda$$
$$F' = 0 \quad \text{on wall:} \quad t_w = -\frac{\tau}{2} F_w^2 \tag{28}$$

F match with quasi-neutral solution $(-\lambda/t)$ as $t \to \infty$ where

$$\lambda = (\bar{J}_+ - \bar{J}_-) / (\bar{J}_+ + \tau \bar{J}_-)$$

Equation (28) has been discussed and solved in Ref. 4 with a tabulation of numerical data for constructing probe characteristics given in Ref. 10. The $\bar{J}_\pm$ are related

to $J_\pm = \Gamma_{w\pm} r_p/D_\pm N_o$ (the particle currents received by the probe normalized by the appropriate random thermal current[4]) by

$$\bar{J}_\pm = \zeta_s^2 J_\pm \tag{29}$$

3. Matching Quasi-Neutral and Sheath Regions

The quasi-neutral solution as $\zeta \to \zeta_s$ must match with the sheath solution as $t \to \infty$. The overlap occurs for $\zeta - \zeta_s > O(\rho_p^{-2/3})$ or $t < O(\rho_p^{2/3})$, e.g. $\zeta - \zeta_s = O(\rho_p^{-1/3})$ and $t = O(\rho_p^{1/3})$ is within the overlap domain. This matching gives

$$c_2 = \left\{ \frac{J_+ + \tau J_-}{1+\tau} \zeta_s^2 + A\left[\frac{1}{2\zeta_s^2} \left(\frac{1+\tau}{J_+ + \tau J_-} \right) - \frac{2}{\zeta_s^2} \left(\frac{1+\tau}{J_+ + \tau J_-} \right) \ln \left| \frac{(1+\tau)\zeta_s^{-2}}{J_+ + \tau J_-} \right| \right] \right\}^{-1} \tag{30}$$

and

$$c_3 = c_2 \left\{ - \frac{J_+ - J_-}{J_+ + \tau J_-} + A\left[\frac{J_+ - J_-}{J_+ + \tau J_-} \left(\frac{-1}{2\zeta_s^2} \right) + \frac{1-\delta}{1+\tau\delta} \frac{1}{2\zeta_s^2} \right] \right\} \tag{31}$$

where ζ_s is given in terms of c_2 in Eq. (24).

We have now the complete solution for n_+, n_- and $d\psi/d\zeta$ and can combine all this and form current-voltage characteristics for spherical probes in a slightly ionized, collision-dominated gas with weak production.

D. Current-Voltage Characteristics

Since the integration of Eq. (28) is done for fixed λ, we wish to express J_+, J_-, and ψ_p in terms of the parameter λ. From the tabulation of Ref. 10, $t_w(\lambda, \tau)$ is known and this is expressed in terms of J_+, J_- via Eqs. (25 and 27). Hence

$$t_w = -\rho_p^{2/3} \; (1 - \zeta_s) \, \zeta_s^{-4/3} \, (J_+ + \tau J_-)^{1/3} \tag{32}$$

Since t_w is finite, this proves that $1 - \zeta_s = O(\rho_p^{-2/3})$. Now ζ_s is given in terms of J_+ and J_- through Eqs. (24 and 30). Thus, to order $\rho_p^{-2/3}$, we have

$$\frac{J_+ + \tau J_-}{1 + \tau} = 1 - \frac{t_w}{\rho_p^{-2/3}(1 + \tau)^{1/3}} \quad (1 + A) + O(\rho_p^{-4/3}) \tag{33}$$

Together with the definition of λ, this yields

$$J_+ = (1 + \lambda \tau) \, [\, 1 - W \, (1 + A) \,] \tag{34}$$

$$J_- = (1 - \lambda) \, [\, 1 - W \, (1 + A) \,] \tag{35}$$

where

$$W = t_w / \, [\rho_p^{2/3} \; (1 + \tau)^{1/3}] < 0 \tag{36}$$

In terms of W, we have

$$\zeta_s = 1 + W \tag{37}$$

$$c_2 = [1 + W + \frac{1}{2} A + \frac{1}{2} \; WA \,]^{-1} = [\, (1 + W) \; (1 + \frac{A}{2}) \,]^{-1} \tag{38}$$

$$c_3 = c_2 \{ -\lambda + A \, [-\lambda(\frac{1}{2} - W) + \frac{1 - \delta}{1 + \tau\delta} \; (\frac{1}{2} - W)] \, \} \tag{39}$$

Now ψ_p is expressed as a function of λ by

$$-\psi_p = \int_0^1 \frac{d\psi}{d\zeta} \, d\zeta = \int_{\text{wall}}^{\text{sheath edge}} \frac{d\psi}{d\zeta} \, d\zeta + \int_{\text{sheath edge}}^{\zeta^*} \frac{d\psi}{d\zeta} \, d\zeta + \int_{\zeta^*}^{0} \frac{d\psi}{d\zeta} \, d\zeta \tag{40}$$

$$\equiv I_1 \qquad + I_2 \qquad + I_3$$

where ζ^* is within the overlap domain of the main quasi-neutral region and the distant quasi-neutral region. The sheath edge is in the overlap domain of the sheath and main quasi-neutral region. Now,

$$I_1 = -\int_{t_w(\lambda,\tau)}^{t_{ms}(\lambda,\tau)} F\,(t;\,\lambda,\tau)dt = -S(\lambda,\tau)$$

as in Ref. 10. For the limits on I_2, we have $\zeta\,(t_{ms}) = \zeta_{ms} = 1 + W - \frac{t_{ms}}{t_w} W$ and ζ^* respectively and the integrand is given by Eq. (18). The integrand of I_3 is Eq. (23). We observe that the first term is a perfect differential and the second (with $\bar{c}_3$ in the numerator) may be expanded by the binomial theorem and then integrated in terms of exponential integral functions. We use the earlier results that $c_1 = 1$ and $\bar{c}_3 = c_3 + B\,c_2/A$. Thus, we obtain $\psi_p(\lambda,\tau) = S\,(\lambda,\tau) + \psi\,(\zeta_{ms})$ where $-\psi\,(\zeta_{ms}) = I_2 + I_3$. Now

$$\psi_p = S(\lambda,\tau) - \frac{c_3}{c_2}\ln(1 - c_2\,\zeta_{ms}) + A\left\{-\frac{1-\delta}{1+\tau\delta}\cdot\frac{c_2}{2\,\zeta_{ms}} + \right.$$

$$\left[\frac{1-\delta}{1+\tau\delta}\cdot\frac{c_2^2}{2} + \frac{c_2 c_3}{2}\right]\ln\left(\frac{1}{\zeta_{ms}} - c_2\right) + \left(\frac{c_2^2 c_3\,\zeta_{ms}}{1 - c_2\,\zeta_{ms}} + c_2 c_3\right)\ln\zeta_{ms}$$

$$\left. + \frac{c_2^2\,c_3}{2}\;\frac{\zeta_{ms}}{1 - c_2\,\zeta_{ms}}\right\} + K \tag{41}$$

where $K = \left[(1-\delta)/(1+\tau\delta)\right]\left\{c_2 A^{1/2} + c_2^2\,A\left[\ln(2A^{1/2}) + \gamma - 2.5\right]\right\} + O(A^{3/2})$. Note that the contribution from the lower limit ζ^* on I_3 cancels with the contribution from the upper limit of I_2 provided that ψ has been matched in the overlap domain between the two regions. It is this matching which determines the constant of integration K.

Likewise, the electrical current to the wall may be written

$$I = 4\pi r_p^2 e(\Gamma_{+w} - \Gamma_{-w}) = 4\pi r_p e D_- N_o \ (\delta J_+ - J_-)$$

Using Eqs. (34) and (35),

$$I = 4\pi r_p e D_- N_o [(1 + \delta\tau)\lambda - (1 - \delta)][1 - W(1 + A)] \tag{42}$$

The differences among the current voltage characteristics for small A and those for A = 0 are so small that the curves for the several values of A cannot be separated by more than a few line widths and would not be visible in small scale reproduction. Therefore, we have chosen to plot the differences in J_+, J_-, ψ_p between their values at a given A and the values where A = 0. These have all been plotted versus λ, the basic parameter of the problem.

Now $\quad J_+(A) - J_+(0) = -(1 + \lambda\tau)WA$

and $\quad J_-(A) - J_-(0) = -(1 - \lambda)WA$.

Since $W \leq 0$, we see that production increases both the normalized ion and electron currents to the probe at all values of λ (i.e., for all probe potentials ψ_p) by an amount proportional to the production parameter A. Fig. 1 shows $J_+(A) - J_+(0)$, and $J_-(A) - J_-(0)$ vs. λ for $\tau = 1$, $\rho_p = 400$ and A = 0.1, 0.05, 0.01. At $\lambda = 0$, W = 0 so $J_\pm(A) - J_\pm(0) = 0$. This is why the curves look singular on the logarithmic scale. Fig. 2 shows the effect of ρ_p on $J_\pm(A) - J_\pm(0)$ vs. λ. As the ratio of probe size to Debye length ρ_p increases, W decreases by $\rho_p^{-2/3}$ so all current differences are reduced by this factor. Fig. 2 is plotted for $\rho_p = 1600$ and $\tau = 1$. In Fig. 3, we show the effect of τ; the current differences are plotted for $\tau = 10$, $\rho_p = 400$. The symmetry with respect to $\pm\lambda$ is destroyed when $\tau \neq 1$. The ion currents are increased by an increase in τ but the electron currents are only weakly affected. Note the change in the scale of λ at the ends in all the figures. In Figures 4-6, we show the differences due to production of the dimensionless current $J_+ - J_-/\delta$ and probe potential ψ_p vs. λ. The effects of changes in τ and ρ_p are made evident by comparison of Fig. 5 (with $\rho_p = 1600$) with Fig. 4 (with $\rho_p = 400$) and

by comparison of Fig. 6 (with $\tau = 10$) with Fig. 4 (with $\tau = 1$).

In all figures, the ratio of diffusion coefficients δ was taken to be 0.01.

In Figures 7-9, we have plotted J_+ and J_- vs. ψ_p for $A = 0$ and $A = .1$. The maximum relative effect of A is seen to be at most somewhat larger than O(A). Eq. (41) predicts an effect of $O(A^{1/2})$ in $\psi_p(\lambda)$ but the $J_+(\psi_p)$, $J_-(\psi_p)$ curves show a somewhat smaller effect in general. Variations in τ and ρ_p have the same effect as in Ref. 4. Figures 10-12 show $\bar{I} = J_+ - J_-/\delta$ vs. ψ_p for $A = 0$ and $A = .1$. For $\tau = 1$ (Figs. 10 and 11), we predict from the theory that the inflection point should occur at $\lambda = 0$ to order $\rho_p^{-2/3}$. For $\tau = 10$ (Fig. 12), we predict that the inflection point should occur slightly to the right of $\lambda = 0$. On all three figures, $\lambda = 0$ occurs near $\psi_p = 0$. The $\lambda = 0$ point has significance in our proposed sequence of measurements for the experimentalist. See Section E.

E. Application to Measurements

From Eqs. (41) and (42), we can construct a procedure for measuring in sequence D_-N_o, $\tau = T_-/T_+$, $\delta = D_+/D_-$, and A or α, the normalized recombination rate coefficient.

By differentiating Eq. (41) twice in the case W = 0 (or $\rho_p = \infty$) and using Eq. (42) for $\lambda(I)$, we find that the inflection point on the $I - \psi_p$ characteristic is given by

$$\frac{d^2 \psi_p}{d \bar{I}^2} = \frac{d^2 S}{d \bar{I}^2} + O(W) = \left(\frac{1}{1 + \delta \tau}\right)^2 \frac{d^2 S}{d \lambda^2} = 0$$

where $\bar{I} = I/(4 \pi r_p e D_- N_o)$. To this order, the location of the inflection point is independent of A and determined entirely by the sheath solution (through S) even though in this limit the sheath has zero thickness. Assuming a priori that the inflection point occurs for small λ, we find that

$$\lambda = - \frac{\tau - 1}{\tau} \frac{b}{f_w^3} \quad \text{for inflection}$$

where $f_w^3 = 2.148$ and f is defined in Appendix A, and b is a numerical constant obtained by an integral of the second order small λ solution (the first order of which is given in Appendix A). We crudely estimate b as about 0.3. Thus for $\tau = 1$, the inflection point occurs at $\lambda = 0$ and for all $\tau > 1$, the inflection point occurs for small negative λ. Using this information, the experimenter may approximate the $\lambda = 0$ point on the current-voltage characteristic. Since $\frac{\tau - 1}{\tau}$ is at most equal to 1.0 for large τ, the error in λ is numerically about .02. The point of inflection occurs in a region of smooth behavior of I vs. ψ_p so that a small numerical error in λ represents a corresponding small numerical error in the current I. When $\lambda = 0$, $J_+ = J_- = 1$ and we define the following sequence of measurements.

$$I(\lambda = 0) = -4\pi r_p e D_- N_o (1 - \delta) [1 + O(\rho_p^{-2/3})] \tag{43}$$

Since $\delta = D_+/D_-$ is very small (10^{-2}) when electrons carry the negative charge, Eq. (43) gives us a direct measurement of the product D_-N_o. Using this, we now

measure current for $\psi_p \to \infty$ $(\lambda \to -1/\tau)$:

$$I(\psi_p \to \infty) = -4\pi r_p \, e D_- N_o \, (1 + 1/\tau) \, [\, 1 + O(\rho_p^{-2/3}) \,] \tag{44}$$

This gives us $\tau = T_-/T_+$ since $D_- N_o$ is already known. The limiting current for $\psi_p \to -\infty$ $(\lambda \to 1)$ is

$$I(\psi_p \to -\infty) = 4\pi r_p \, e D_- N_o \, \delta \, (1 + \tau) \, [\, 1 + O(\rho_p^{-2/3}) \,]. \tag{45}$$

Eq. (45) now gives a direct measurement of $\delta = D_+/D_-$. We may make one more measurement quite easily, the slope of the current-voltage characteristic at the $\lambda = 0$ point.

$$\left(\frac{dI}{d\varphi_p}\right)_{\lambda=0} = \frac{e}{kT_-}\left(\frac{dI}{d\psi_p}\right)_{\lambda=0} = \frac{e}{kT_-}\left(\frac{dI}{d\lambda}\right)_{\lambda=0}\left(\frac{d\lambda}{d\psi_p}\right)_{\lambda=0}$$

$$= 4\pi r_p \, \frac{e^2 D_- N_o}{kT_-}\left\{\frac{(1+\delta\tau)}{\left(\frac{d\psi_p}{d\lambda}\right)_{\lambda=0}} + O(\rho_p^{-2/3})\right\}.$$

Now,

$$\left(\frac{d\psi_p}{d\lambda}\right)_{\lambda=0} = G + \ln\left(\frac{A}{2} + \bar{W}\right) - \frac{A\bar{W}}{A + 2\bar{W}} - \frac{A - A^2 - 3A\bar{W}}{A + 2\bar{W} - A\bar{W}}$$

where $G = \left(\frac{dS}{d\lambda}\right)_{\lambda=0}$ is a universal constant discussed in the Appendix A and where $\bar{W} = t_{ms}(1+\tau)^{-1/3} \rho_p^{-2/3} > 0$.

$$\left(\frac{dI}{d\varphi_p}\right)_{\lambda=0} = 4\pi r_p \, \frac{e^2 D_- N_o}{kT_-}\left\{(1+\delta\tau)\left[G + \ln\left(\frac{A}{2} + \bar{W}\right) - \frac{A\bar{W}}{A+2\bar{W}} - \frac{A - A^2 - 3A\bar{W}}{A + 2\bar{W} - A\bar{W}}\right]^{-1}\right\} \tag{46}$$

If T_+ is regarded as known (equal to the gas temperature, say) then knowing τ gives us T_- and Eq. (46) then gives us a measurement of A or α, the normalized recombination

rate coefficient. All the proposed measurements above are given with relative errors of $O(\rho_p^{-2/3})$. Note that the principal dependence on ρ_p is in the $\ln(\frac{A}{2} + \bar{W})$ term giving the weak $(\ln \rho_p)$ dependence of the slope as in Ref. 4. Moreover, the T_-/N_o occurring in ρ_p through λ_D appears as $\ln(T_-/N_o)^{1/3}$ which is very insensitive to a guess of the quantity T_-/N_o.

F. Conclusions

We have solved the problem of a spherical electrostatic probe in a slightly ionized, collision-dominated gas with weak ionization and recombination by a double asymptotic expansion: ρ_p $(= r_p/\lambda_D) \to \infty$ and A (the production parameter)$\to$ 0. In the double limit, we find three distinct regions: a space charge sheath, a main quasi-neutral region, and a distant quasi-neutral region. Solutions for density and electric field (or potential) are obtained in each region and matched in the overlap domains between regions. From the solutions, current-voltage characteristics may be computed (indirectly). The fractional change in ion and electron currents (for fixed λ) due to a change in A is shown to be $O(A\ \rho_p^{-2/3})$ to lowest order as $A \to 0$ and $\rho_p \to \infty$. However, the fractional change in ψ_p (for fixed λ) due to a change of A is $O(A^{1/2})$. Thus the actual current-voltage characteristics would seem to be shifted by amount of $O(A^{1/2})$ although the actual effect appears to be somewhat smaller.

References

1. Sutton, G. W. and Sherman, A., Engineering Magnetohydrodynamics (McGraw-Hill Book Co., Inc., New York, 1965), p. 168.

2. Delcroix, J.-L., Introduction to the Theory of Ionized Gases, (Interscience Publishers, Inc., New York, 1960), p. 39.

3. Su, C. H. and Lam, S. H., "The Continuum Theory of Spherical Electrostatic Probes," Phys. Fluids 6, 1479-1491 (1963).

4. Cohen, I. M., "Asymptotic Theory of Spherical Electrostatic Probes in a Slightly Ionized, Collision-Dominated Gas," Phys. Fluids 6, 1492-1499 (1963).

5. Cohen, I. M., "Asymptotic Theory of Ellipsoidal Electrostatic Probes in a Slightly Ionized, Collision-Dominated Gas," AIAA J. 5, 63-69 (1967).

6. Su, C. H. and Sonin, A. A., "Theory of the Electrostatic Probe in a Moderately Ionized Gas," Phys. Fluids 10, 124-126 (1967).

7. Chapman, S. and Cowling, T. G., The Mathematical Theory of Nonuniform Gases, (Cambridge University Press, London, 1952), Chapter 9.

8. Whitman, A. M. and Yeh, H., "Characteristics of Plasma Probes in a MHD Working Fluid," Presented at International Symposium on MHD Electrical Power, Salzburg, July 4-6, 1966.

9. Davydov, B. and Zmanovskaja, L., "Zur Theorie Der Elektrischen Sonden in Gasentladungsröhren," Zh. Tekh. Fiz. 28, 715-728 (1936).

10. Cohen, I. M., "Asymptotic Theory of a Photoionization Chamber," Phys. Fluids 8, 2097-2105 (1965).

11. Kruskal, M. D., "Asymptotology," in Mathematical Models in Physical Sciences, Edited by S. Drobot (Prentice-Hall, Inc., Englewood Cliffs, N.J., 1963).

12. Cohen, I. M. and Kruskal, M.D., "Asymptotic Theory of the Positive Column of a Gas Discharge," Phys. Fluids 8, 920-934 (1965), Erratum, Phys. Fluids 9, 1051-1052 (1966).

Appendix A: Evaluation of $S(\lambda, \tau)$ for small λ.

From Equation (20), we may see that $F = O(\lambda)$ when $\lambda \to 0$.

Thus, defining

$$f = F/\lambda,$$

we have the equation

$$f'' - tf = 1$$

$$f' = 0 \quad \text{on} \quad t_w = 0$$

$$f \to -1/t \quad \text{as} \quad t \to \infty$$

where the relative error is $O(\tau\lambda)$ when $\tau \neq 1$ and $O(\tau\lambda^2)$ when $\tau = 1$.

Now $G = \int_0^{t_{ms}} f(t)\,dt$.

Thus $S = \lambda G$ where S is defined under Equation (40) and (for the smallest relative error) $G = -2.847$ for $t_{ms} = 4.192$ from Table I of Reference 10.

Therefore, $\left(\frac{\partial S}{\partial \lambda}\right)_{\lambda=0} = G = -2.847$ and in $\overline{W} = \dfrac{t_{ms}}{(1+\tau)^{1/3}\,\rho_p^{2/3}}$

we must use $t_{ms} = 4.192$.

Appendix B: Tabular Data

We have computed the differences in current and probe potential between those for $A = .01$, $.05$, $.1$ and $A = 0$ as functions of λ for $\tau = 1$, 10, $\rho_p = 400$ and $\tau = 1$, $\rho_p = 1600$ to illustrate the separate effects of τ and ρ_p on the probe characteristics. All computations have been carried out with $\delta = D_+/D_- = 0.01$. The column headed by "CURR (A) - CURR (0)" is the difference given by

$$[J_+(A) - J_-(A)/\delta] - [J_+(0) - J_-(0)/\delta]$$

and this is the difference in the normalized electrical current density to the probe. The column headed by "LAMDA" is lambda (λ).

Nomenclature

A	perturbation parameter $\alpha(1+\delta\tau)/(1+\tau)$
b	numerical constant
B	$\alpha(1-\delta)/(1+\tau)$
c	constants of integration
D	diffusion coefficient
e	charge on an electron
E	scaled electric field $d\psi/dx$
f	F/λ
F	scaled electric field (Eq. (27))
G	S/λ (Appendix)
I	electric current to probe (Eq. (42))
J	number flux to probe normalized by random thermal flux
$\bar{J}$	$\zeta_s^2 J$
k	Boltzmann's constant
K	constant of integration determined by matching
n	dimensionless number density N/N_o
$\bar{n}$	scaled dimensionless number density in sheath: $\rho_p^{2/3} n$
N	number density
O	asymptotic notation $A = O(B)$ as $\epsilon \to 0$ if $\lim_{\epsilon \to 0} \frac{B}{A}$ is bounded.
r	radial coordinate
S	potential drop in sheath $\int_{t_w}^{t_{ms}} F\,dt$
t	scaled coordinate in sheath region $-(\bar{J}_+ + \tau\bar{J}_-)^{1/3} x$
T	temperature
W	$t_w/[\rho_p^{2/3}(1+\tau)^{1/3}]$; $\bar{W} = t_{ms}/[\rho_p^{2/3}(1+\tau)^{1/3}]$
x	scaled sheath coordinate $= \rho_p^{2/3}\zeta_s^{-2}(\zeta - \zeta_s)$

α	production parameter $\nu_r N_n N_o r_p^2/D_+$
γ	Euler's constant: .577. . .
Γ	number flux
δ	diffusion coefficient ratio D_+/D_-
ζ	normalized coordinate r_p/r
λ	ratio of currents $(J_+ - J_-)/(J_+ + \tau J_-)$
λ_D	Debye length $(kT_-/4\pi N_o e^2)^{1/2}$
μ	mobility coefficient
ν_p, ν_r	ionization (production) and recombination rate coefficients, respectively
π	$\int_{-\infty}^{\infty} (1+x^2)^{-1} dx$
ρ_p	r_p/λ_D
τ	temperature ratio T_-/T_+
φ	electrostatic potential
ψ	dimensionless electrostatic potential $e\varphi/kT_-$

Subscripts

0	at $\zeta = 0$ (or $r = \infty$)
1, 2, 3	denoting specific integrals ($I_{1,2,3}$) and constants of integration ($c_{1,2,3}$)
$\pm$	ions (electrons)
ms	location where machine integration was stopped and solution matched to asymptotic form
n	neutrals
p	on probe
s	at singular point
w	at wall (probe)

FIGURE CAPTIONS

Figure 1. Differences in normalized particle currents to probe versus current ratio parameter λ . $\tau = 1$, $\rho_p = 400$. The kinks in the curves for $|\lambda| \geqslant .9$ are due to the changed scale.

Curve 1: $J_-(A = .01) - J_-(A = 0)$. The curve for $A = .1$ is ten times larger.

Curve 2: $J_-(A = .05) - J_-(A = 0)$.

Curve 3: $J_+(A = .01) - J_+(A = 0)$. The curve for $A = .1$ is ten times larger.

Curve 4: $J_+(A = .05) - J_+(A = 0)$.

All of these differences are zero at $\lambda = 0$.

Figure 2. Differences in normalized particle currents to probe versus current ratio parameter λ . $\tau = 1$, $\rho_p = 1600$. The kinks in the curves for $|\lambda| \geqslant .9$ are due to the changed scale.

Curve 1: $J_-(A = .01) - J_-(A = 0)$. The curve for $A = .1$ is ten times larger.

Curve 2: $J_-(A = .05) - J_-(A = 0)$.

Curve 3: $J_+(A = .01) - J_+(A = 0)$. The curve for $A = .1$ is ten times larger.

Curve 4: $J_+(A = .05) - J_+(A = 0)$.

All of these differences are zero at $\lambda = 0$.

Figure 3. Differences in normalized particle currents to probe versus current ratio parameter λ. $\tau = 10$, $\rho_p = 400$. Note the difference between the $\lambda > 0$ scale and the $\lambda < 0$ scale. The kinks in the curves for $\lambda \geq .9$ are due to the changed scale.

Curve 1: $J_-(A = .01) - J_-(A = 0)$. The curve for $A = .1$ is ten times larger.

Curve 2: $J_-(A = .05) - J_-(A = 0)$.

Curve 3: $J_+(A = .01) - J_+(A = 0)$. The curve for $A = .1$ is ten times larger.

Curve 4: $J_+(A = .05) - J_+(A = 0)$.

All of these differences are zero at $\lambda = 0$.

Figure 4. Differences in normalized electrical current and probe potential versus current ratio parameter λ. $\tau = 1$, $\rho_p = 400$, $\delta = .01$. Note the change in scale for $|\lambda| \geq .9$.

Curve 1: $\bar{I}(A = .01) - \bar{I}(A = 0)$, $\bar{I} = J_+ - J_- / \delta$. The curve for $A = .1$ is ten times larger.

Curve 2: $\bar{I}(A = .05) - I(A = 0)$.

Curve 3: $\psi_p(A = .01) - \psi_p(A = 0)$.

Curve 4: $\psi_p(A = .05) - \psi_p(A = 0)$.

Curve 5: $\psi_p(A = .1) - \psi_p(A = 0)$.

Figure 5: Differences in normalized electrical current and probe potential versus current ratio parameter λ . $\tau = 1$, $\rho_p = 1600$, $\delta = .01$. Note the change in scale for $|\lambda| \geq .9$.

Curve 1: $\bar{I}(A = .01) - \bar{I}(A=0)$. $\bar{I} = J_+ - J_-/\delta$. The curve for $A = .1$ is ten times larger.

Curve 2: $\bar{I}(A = .05) - \bar{I}(A = 0)$.

Curve 3: $\psi_p(A = .01) - \psi_p(A = 0)$.

Curve 4: $\psi_p(A = .05) - \psi_p(A = 0)$.

Curve 5: $\psi_p(A = .1) - \psi_p(A = 0)$.

Figure 6: Differences in normalized electrical current and probe potential versus current ratio parameter λ . $\tau = 10$, $\rho_p = 1600$, $\delta = .01$. Note changes in the λ scale.

Curve 1: $\bar{I}(A = .01) - \bar{I}(A = 0)$. $\bar{I} = J_+ - J_-/\delta$. The curve for $A = .1$ is ten times larger.

Curve 2: $\bar{I}(A = .05) - \bar{I}(A = 0)$.

Curve 3: $\psi_p(A = .01) - \psi_p(A = 0)$.

Curve 4: $\psi_p(A = .05) - \psi_p(A = 0)$.

Curve 5: $\psi_p(A = .1) - \psi_p(A = 0)$.

Figure 7: Normalized ion and electron currents to probe versus normalized probe potential for $A = 0$ and $A = .1$. $\tau = 1$, $\rho_p = 400$, $\delta = .01$.

Figure 8: Normalized ion and electron currents to probe versus normalized probe potential for $A = 0$ and $A = .1$. $\tau = 1$, $\rho_p = 1600$, $\delta = .01$.

Figure 9: Normalized ion and electron currents to probe versus normalized probe potential for $A = 0$ and $A = .1$. $\tau = 10$, $\rho_p = 400$, $\delta = .01$.

Figure 10: Normalized electrical current to probe ($\bar{I} = J_+ - J_- / \delta$) versus normalized probe potential for $A = 0$ and $A = .1$. $\tau = 1$, $\rho_p = 400$, $\delta = .01$.

Figure 11: Normalized electrical current to probe ($\bar{I} = J_+ - J_- / \delta$) versus normalized probe potential for $A = 0$ and $A = .1$. $\tau = 1$, $\rho_p = 1600$, $\delta = .01$.

Figure 12: Normalized electrical current to probe ($\bar{I} = J_+ - J_- / \delta$) versus normalized probe potential for $A = 0$ and $A = .1$. $\tau = 10$, $\rho_p = 400$, $\delta = .01$.

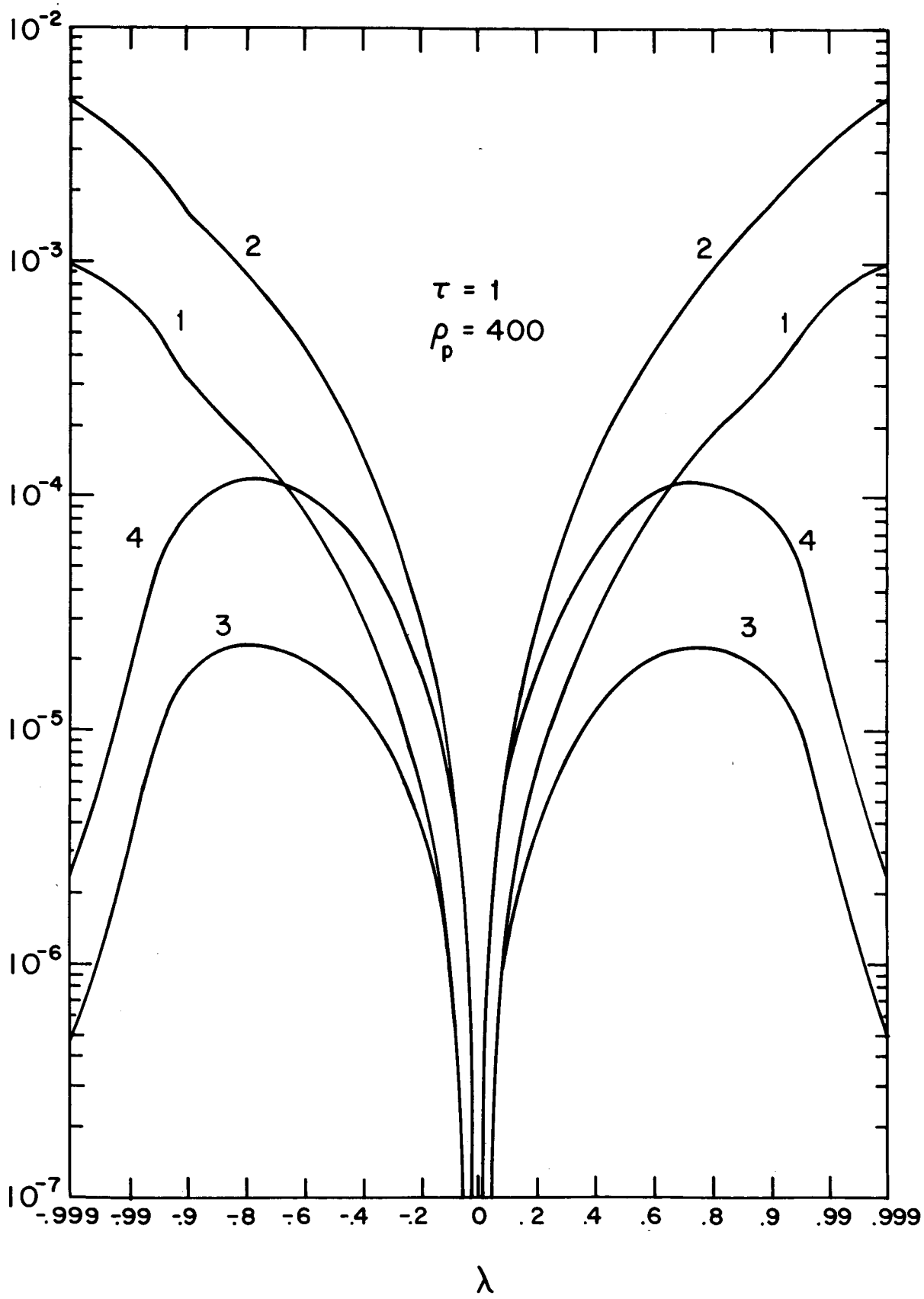
10^{-2}
10^{-3}
10^{-4}
10^{-5}
10^{-6}
10^{-7}
$\tau = 1$
$\rho_p = 400$
1
2
3
4
-.999 -.99 -.9 -.8 -.6 -.4 -.2 0 .2 .4 .6 .8 .9 .99 .999
λ

FIG. 1

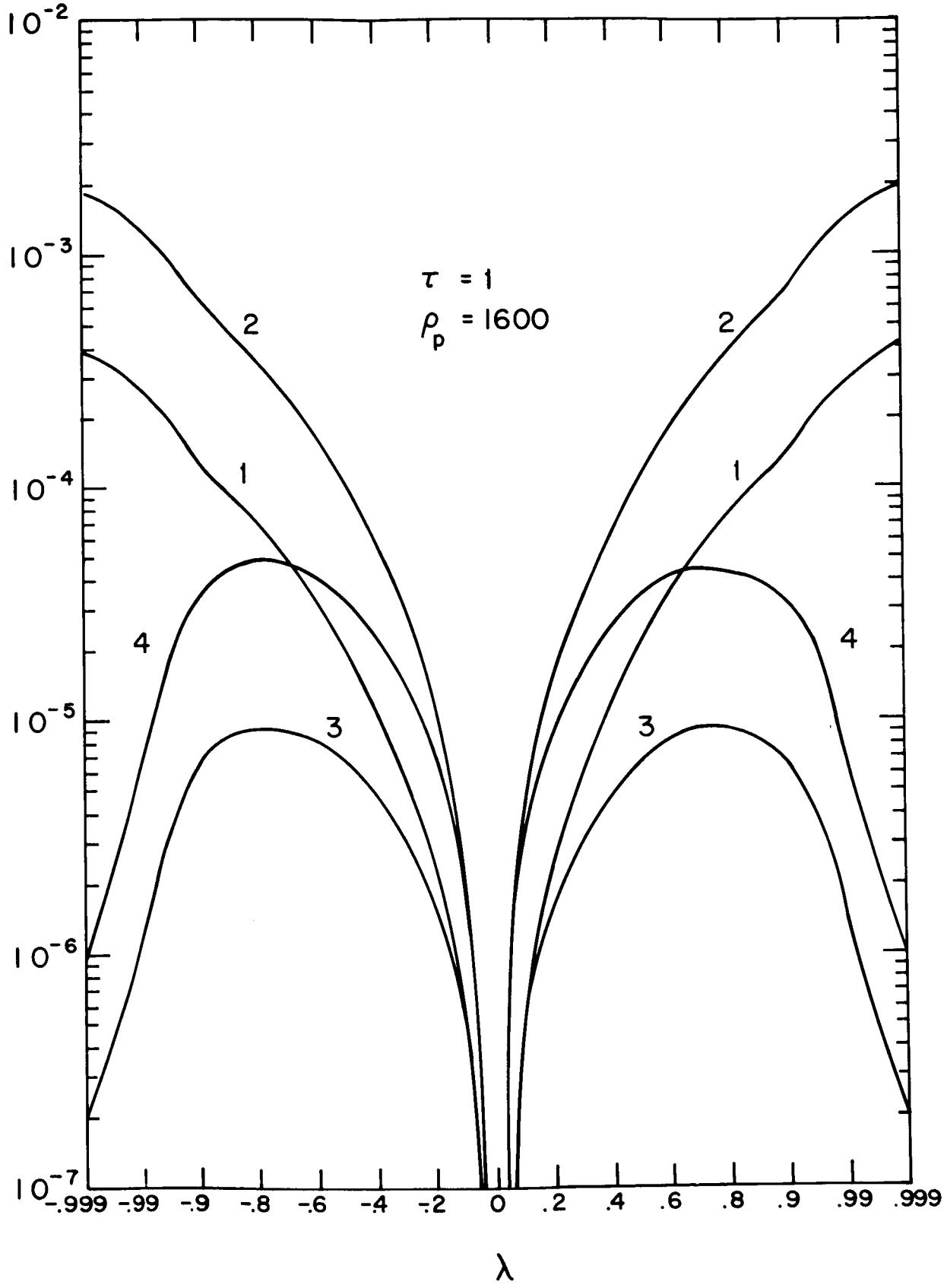
10^{-2}
10^{-3}
10^{-4}
10^{-5}
10^{-6}
10^{-7}
$\tau = 1$
$\rho_p = 1600$
1
2
3
4
-.999 -.99 -.9 -.8 -.6 -.4 -.2 0 .2 .4 .6 .8 .9 .99 .999
λ

FIG. 2

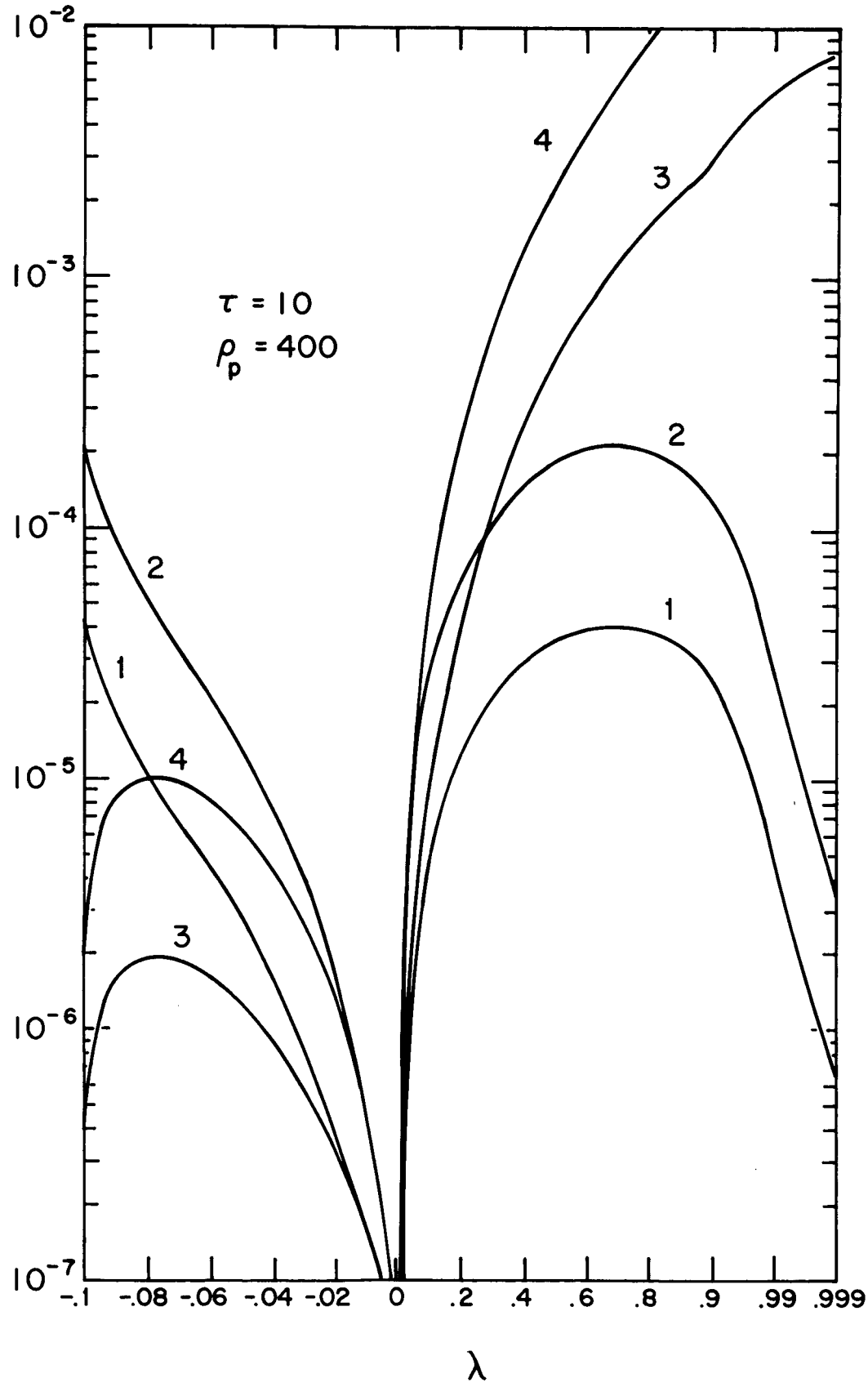
10^{-2}
10^{-3}
10^{-4}
10^{-5}
10^{-6}
10^{-7}
$\tau = 10$
$\rho_p = 400$
1
2
3
4
-.1
-.08
-.06
-.04
-.02
0
.2
.4
.6
.8
.9
.99
.999
λ

FIG. 3

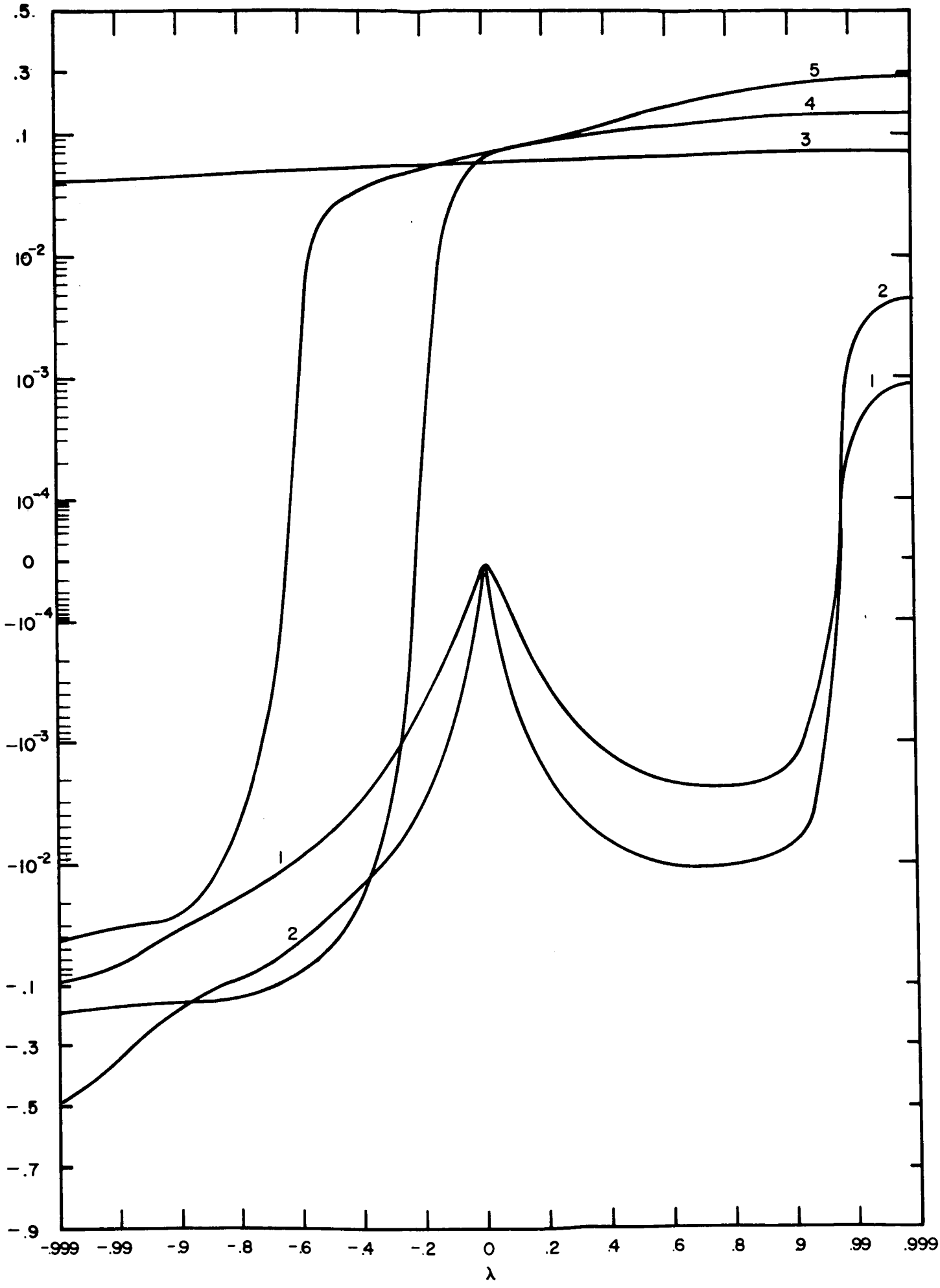
.5
.3
.1
10^{-2}
10^{-3}
10^{-4}
0
-10^{-4}
-10^{-3}
-10^{-2}
-.1
-.3
-.5
-.7
-.9
-.999
-.99
-.9
-.8
-.6
-.4
-.2
0
.2
.4
.6
.8
.9
.99
.999
λ
1
2
3
4
5

FIG. 4

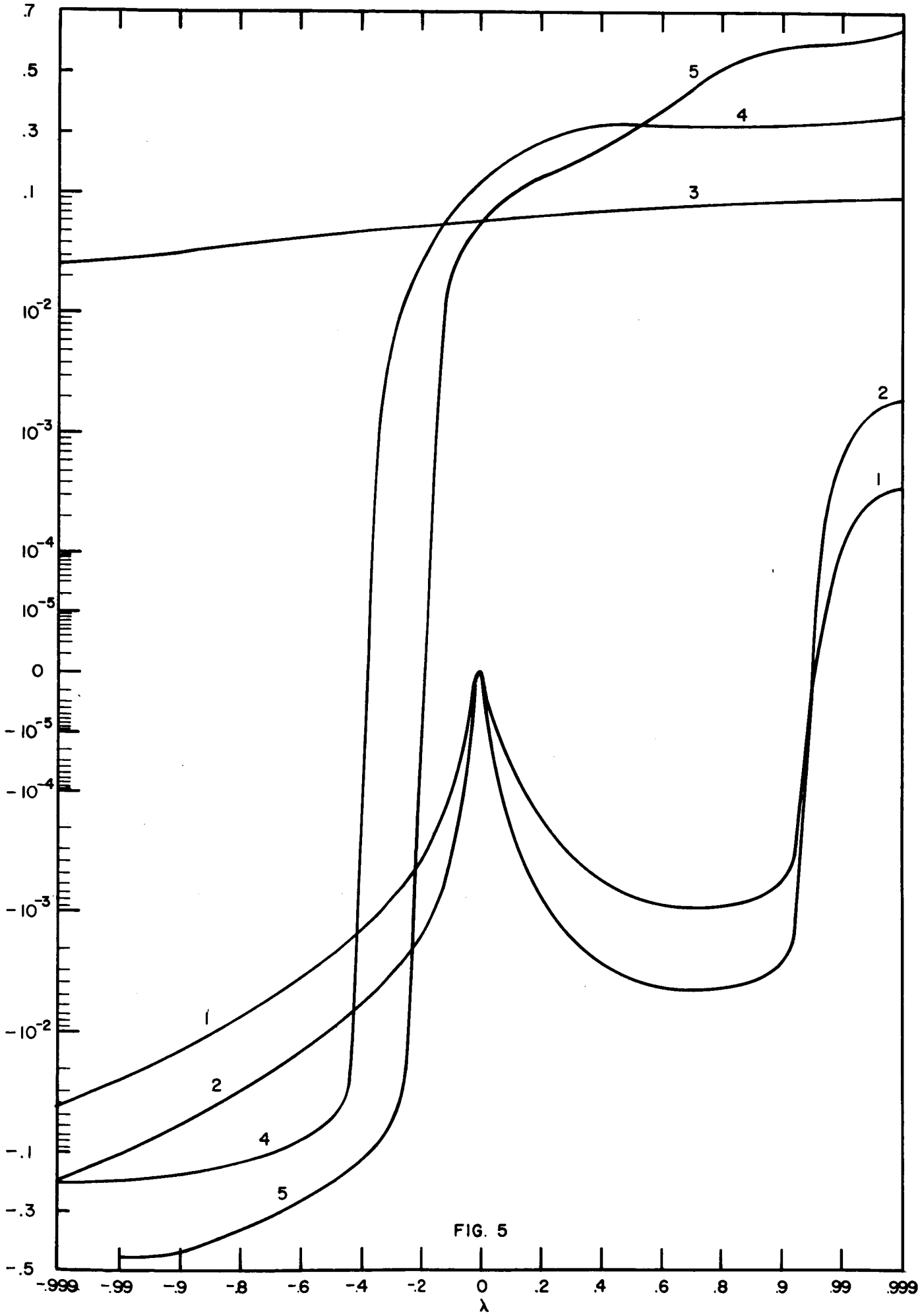
.7
.5
.3
.1
10^{-2}
10^{-3}
10^{-4}
10^{-5}
0
-10^{-5}
-10^{-4}
-10^{-3}
-10^{-2}
-.1
-.3
-.5
-.999
-.99
-.9
-.8
-.6
-.4
-.2
0
.2
.4
.6
.8
.9
.99
.999
λ
1
2
3
4
5

FIG. 5

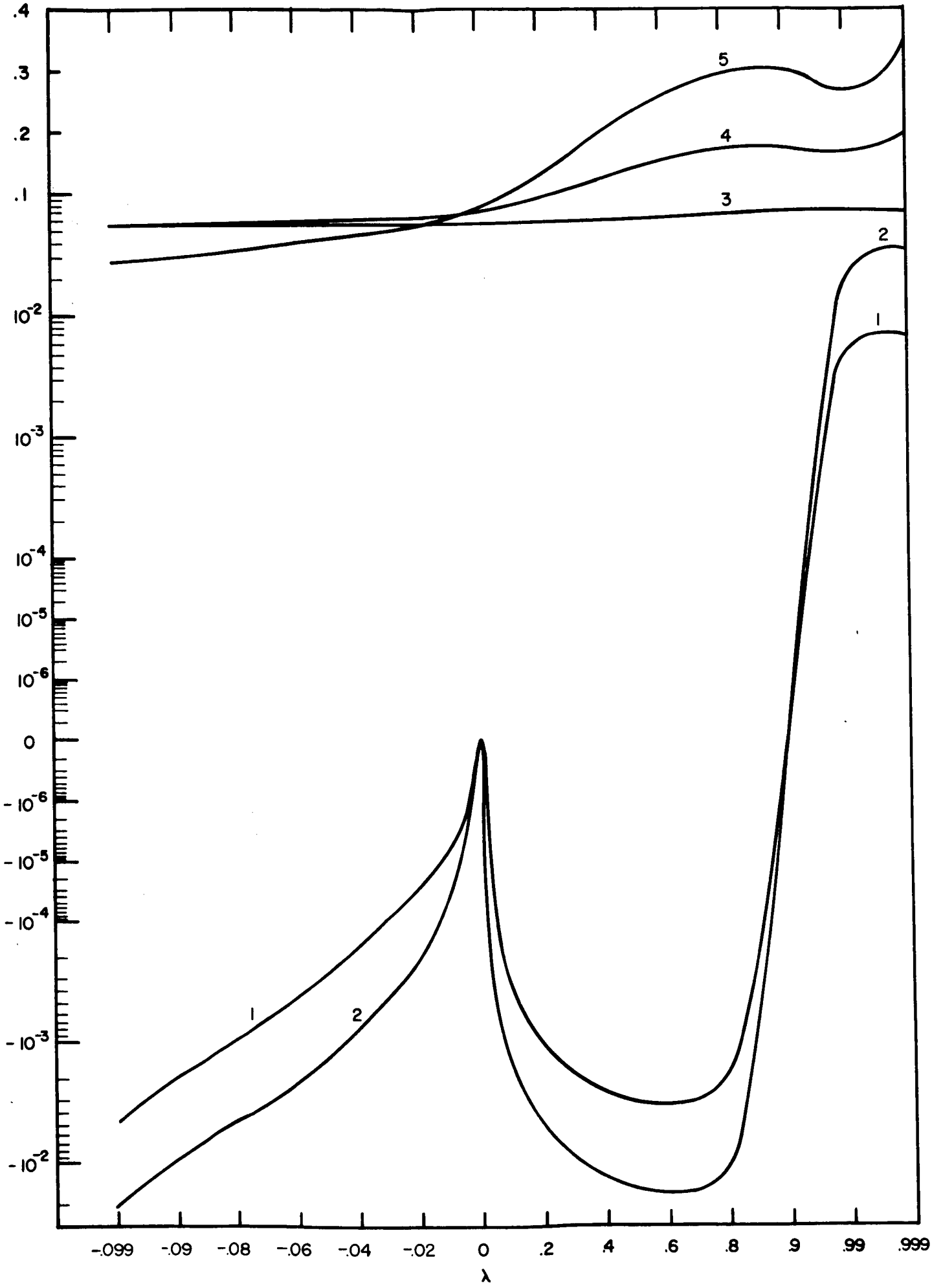
.4
.3
.2
.1
10^{-2}
10^{-3}
10^{-4}
10^{-5}
10^{-6}
0
-10^{-6}
-10^{-5}
-10^{-4}
-10^{-3}
-10^{-2}
5
4
3
2
1
1
2
-.099
-.09
-.08
-.06
-.04
-.02
0
.2
.4
.6
.8
.9
.99
.999
λ

FIG. 6

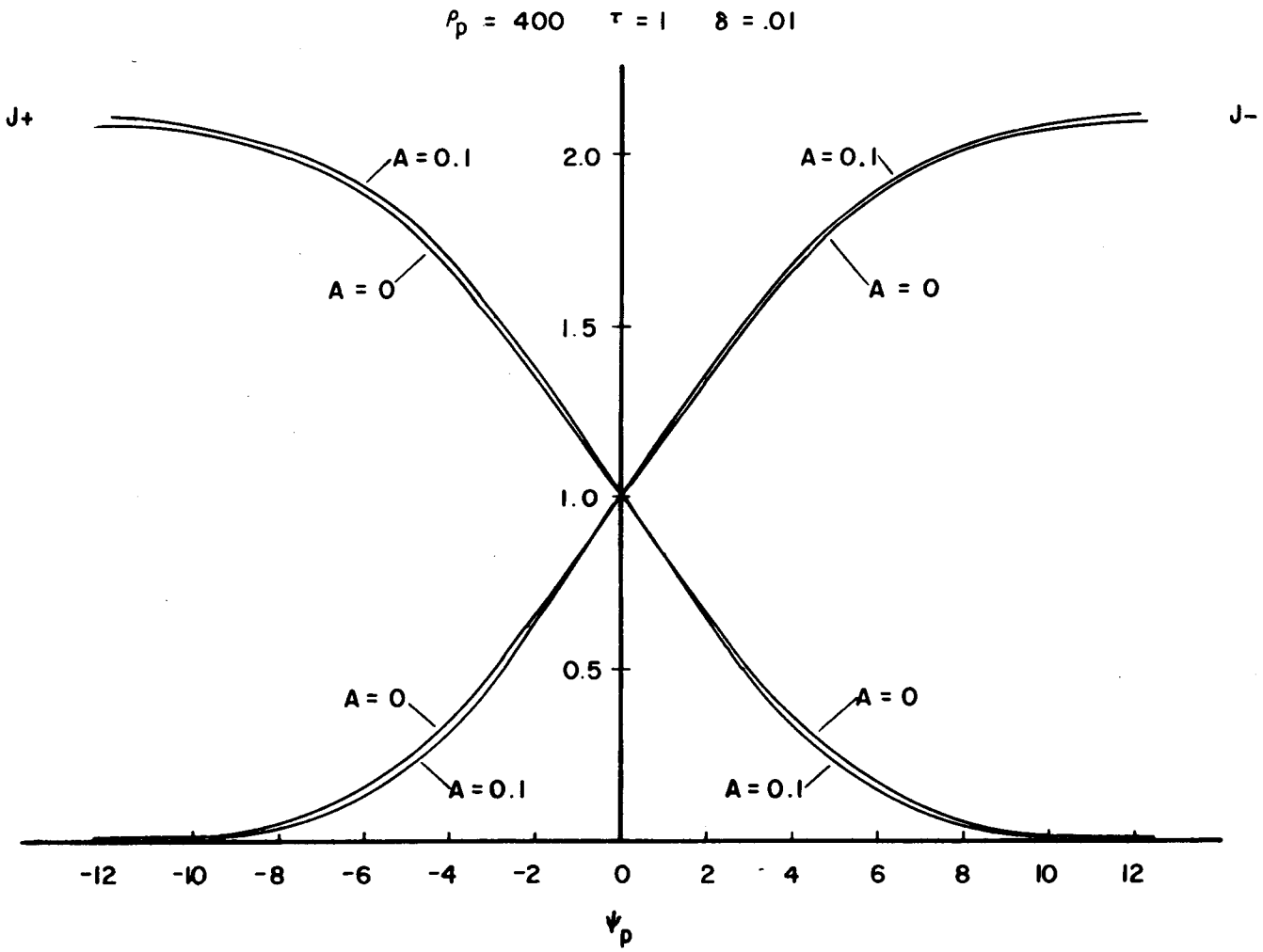
ρ_p = 400 τ = 1 δ = .01
J+
J-
A = 0.1
A = 0
A = 0.1
A = 0
A = 0
A = 0.1
A = 0
A = 0.1
2.0
1.5
1.0
0.5
-12
-10
-8
-6
-4
-2
0
2
4
6
8
10
12
ψ_p

FIG. 7

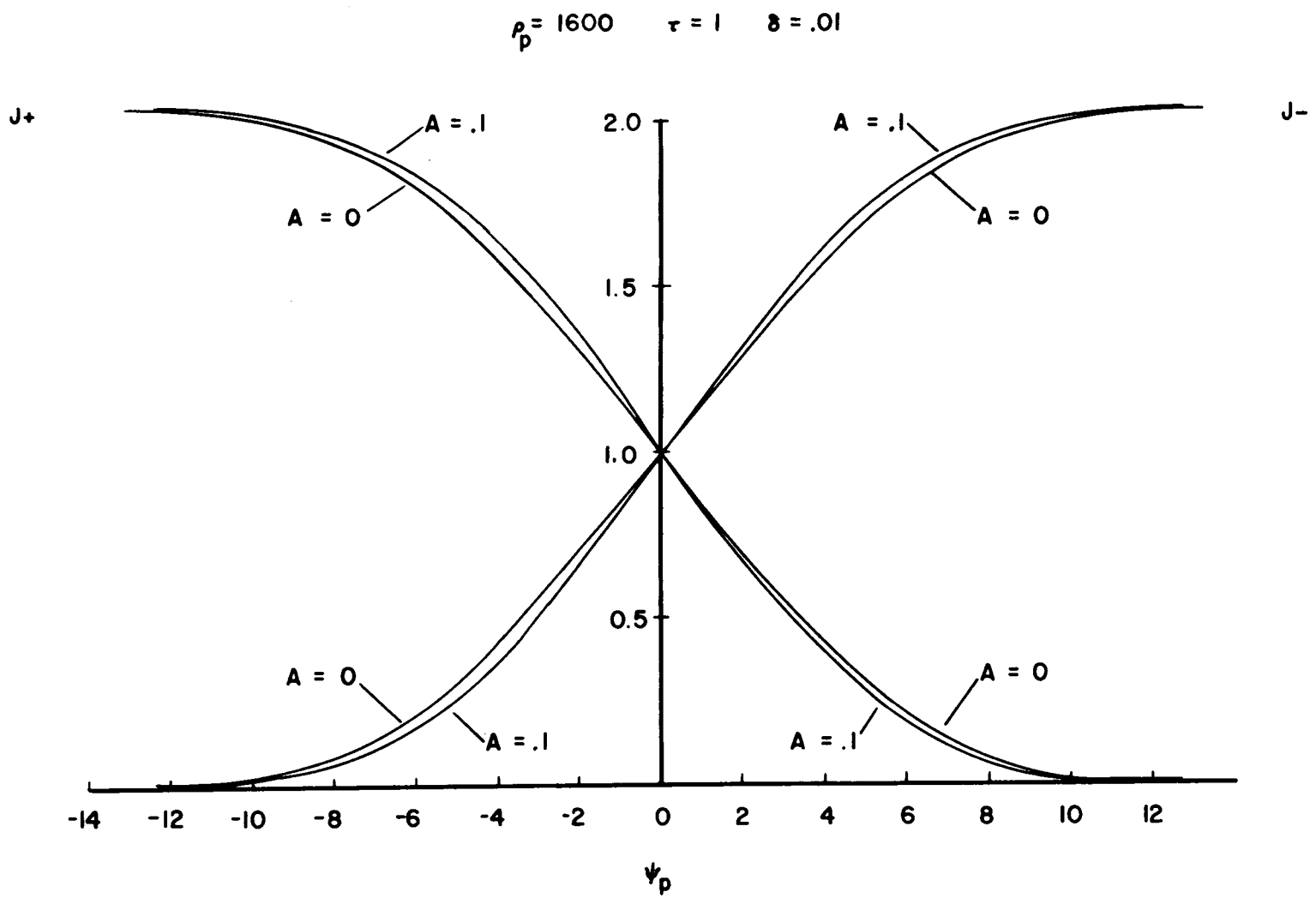
$\rho_p = 1600$ $\tau = 1$ $\delta = .01$
J+
J-
A = .1
A = 0
A = .1
A = 0
A = 0
A = .1
A = .1
A = 0
2.0
1.5
1.0
0.5
-14
-12
-10
-8
-6
-4
-2
0
2
4
6
8
10
12
ψ_p

FIG. 8

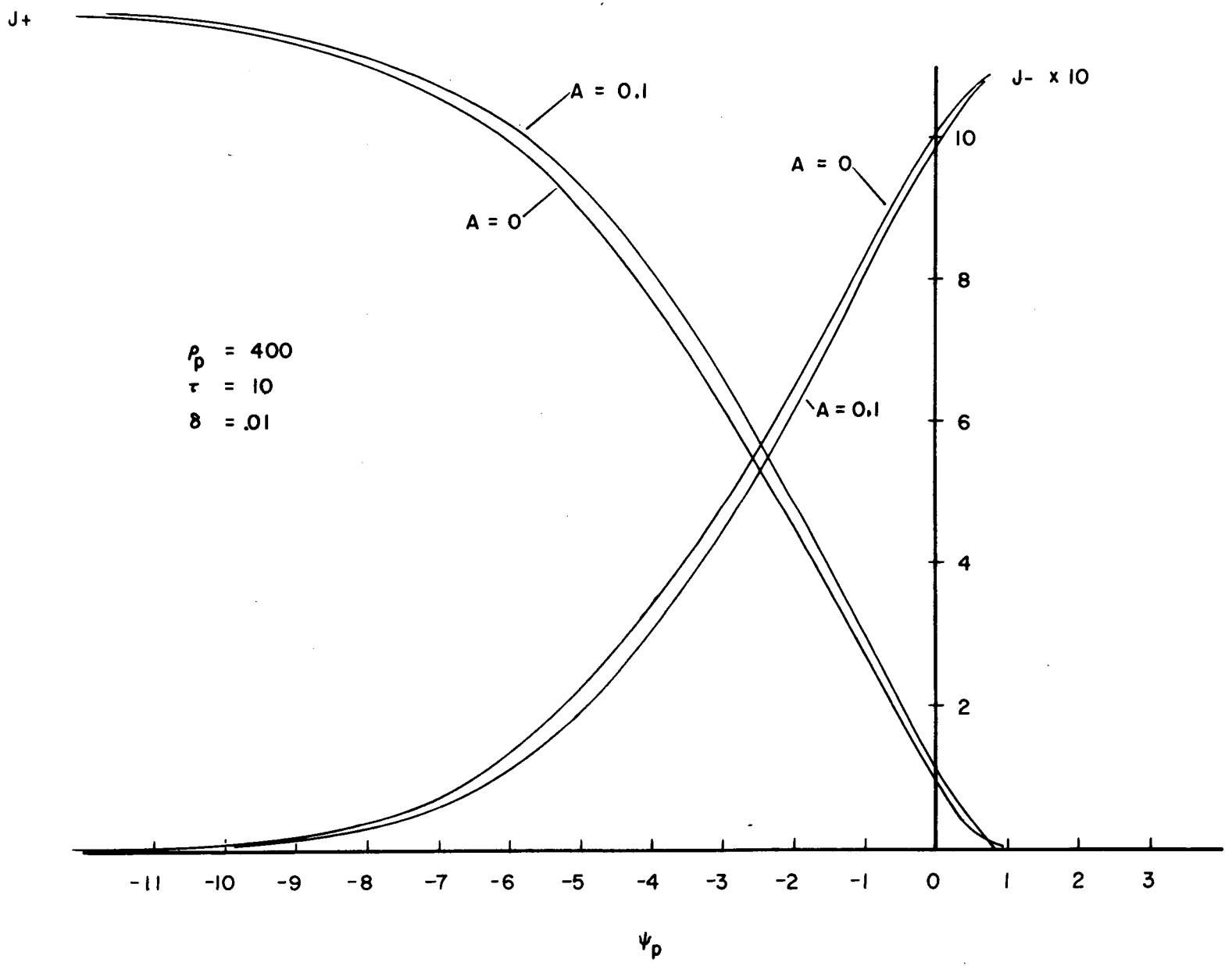
J+
J- x 10
A = 0.1
A = 0
A = 0
A = 0.1
ρ_p = 400
τ = 10
δ = .01
10
8
6
4
2
-11
-10
-9
-8
-7
-6
-5
-4
-3
-2
-1
0
1
2
3
ψ_p

FIG. 9

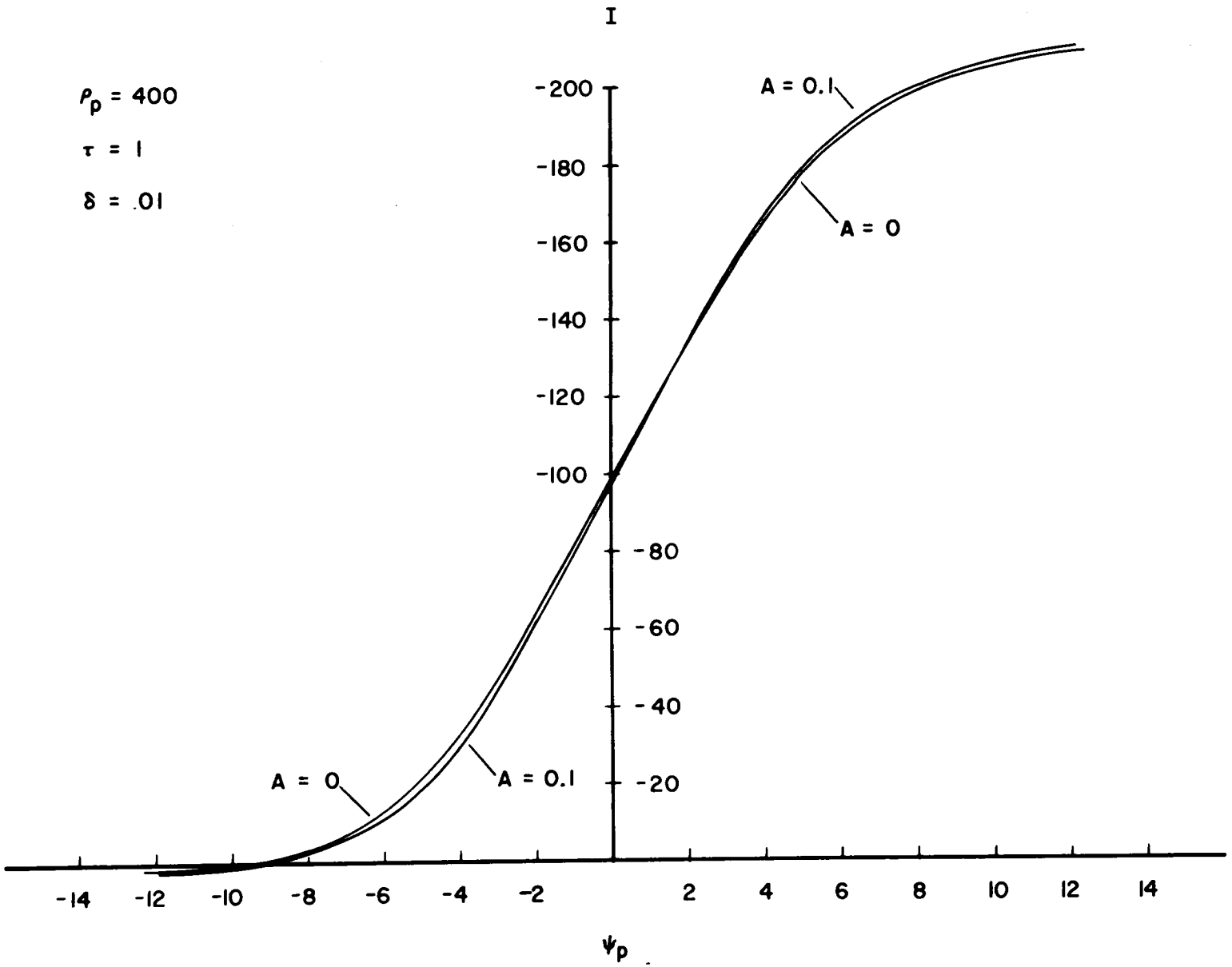
I
ρ_p = 400
τ = 1
δ = .01
-200
-180
-160
-140
-120
-100
-80
-60
-40
-20
A = 0.1
A = 0
A = 0
A = 0.1
-14
-12
-10
-8
-6
-4
-2
2
4
6
8
10
12
14
ψ_p

FIG. 10

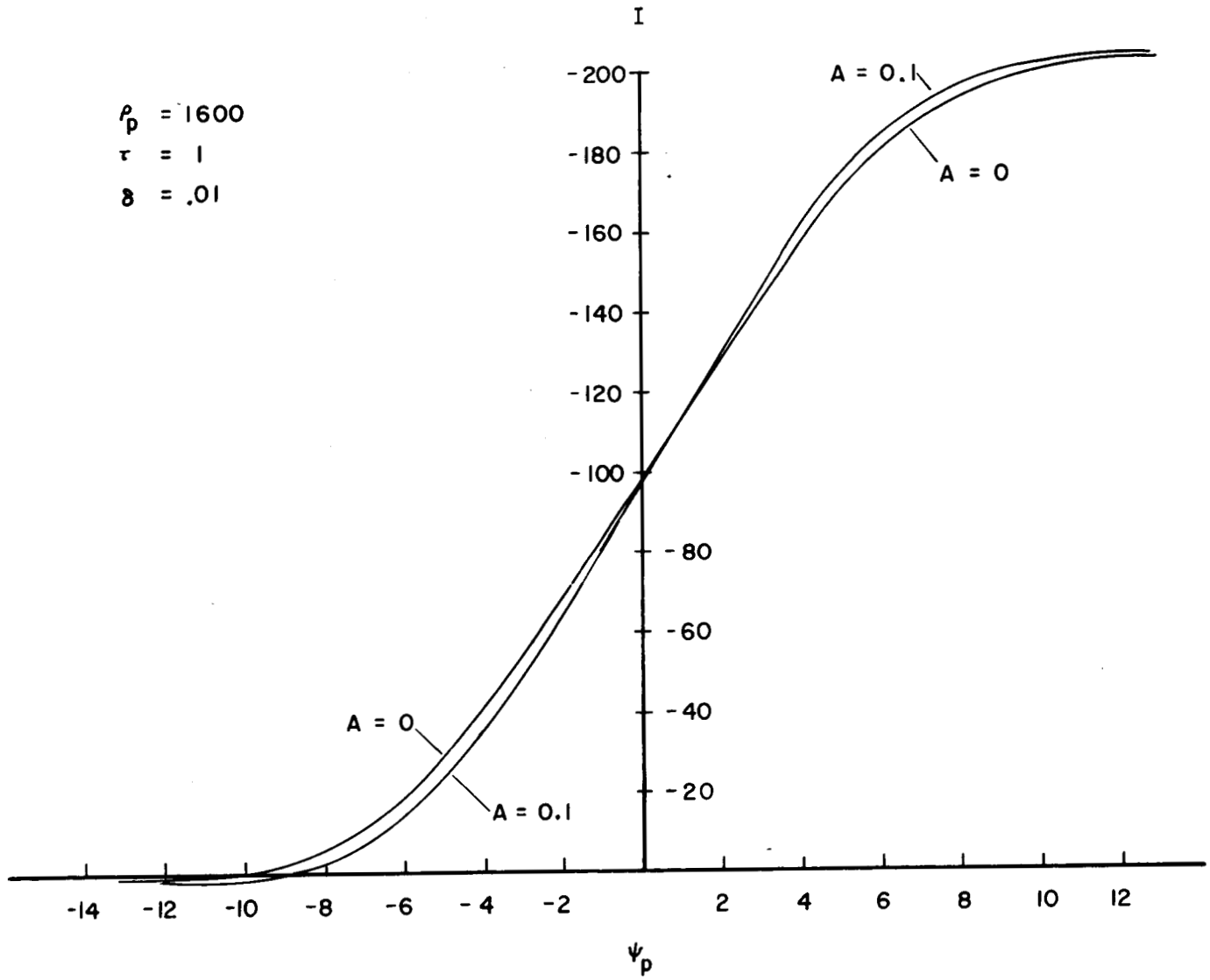
I
ρ_p = 1600
τ = 1
δ = .01
-200
-180
-160
-140
-120
-100
-80
-60
-40
-20
A = 0.1
A = 0
A = 0
A = 0.1
-14
-12
-10
-8
-6
-4
-2
2
4
6
8
10
12
ψ_p

FIG. 11

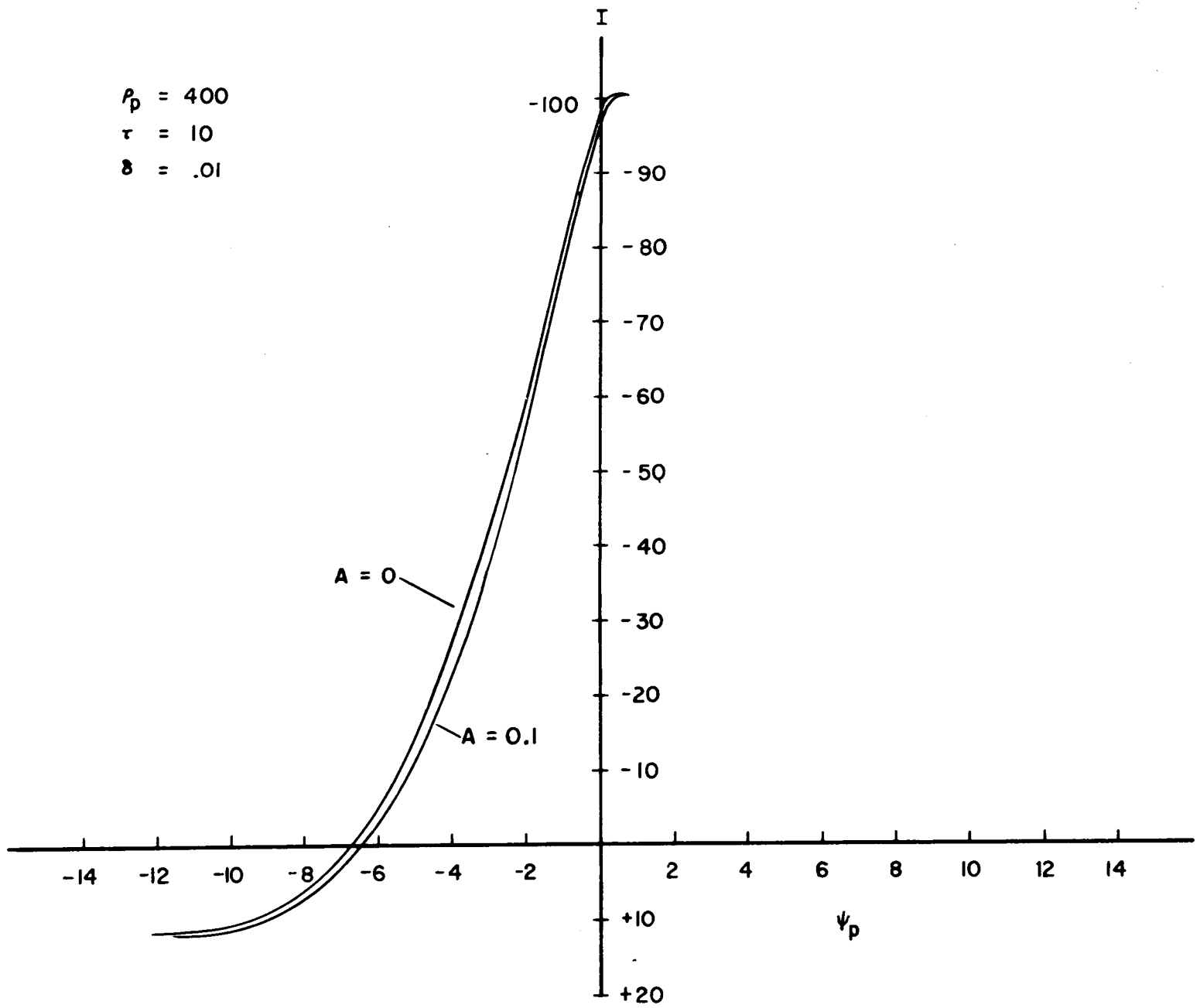
ρ_p = 400
τ = 10
δ = .01
I
-100
-90
-80
-70
-60
-50
-40
-30
-20
-10
+10
+20
A = 0
A = 0.1
-14
-12
-10
-8
-6
-4
-2
2
4
6
8
10
12
14
ψ_p

FIG. 12

APPENDIX B: TABLE 1

A = .01, RHOP = 400, TAU = 1, DELTA = .01

LAMDA	J+(A) - J+(0)	J-(A) - J-(0)	CURR(A) - CURR(0)	PSIP(A) - PSIP(0)
0.99900000E 00	0.97438693E-03	0.48743095E-06	0.92564523E-03	0.75085402E-01
0.98999999E 00	0.68777800E-03	0.34561381E-05	0.34216046E-03	0.73473215E-01
0.90000000E 00	0.32666326E-03	0.17193146E-04	-0.13926029E-02	0.71767867E-01
0.70000000E 00	0.12955070E-03	0.22862107E-04	-0.21567345E-02	0.68333447E-01
0.50000000E 00	0.50768256E-04	0.16920269E-04	-0.16407967E-02	0.65126300E-01
0.30000000E-00	0.14722347E-04	0.79274178E-05	-0.77724457E-03	0.62495962E-01
0.10000000E-00	0.13411045E-05	0.10952353E-05	-0.10776520E-03	0.59947208E-01
-0.10000000E-00	0.10952353E-05	0.13411045E-05	-0.13256073E-03	0.57518221E-01
-0.30000000E-00	0.79274178E-05	0.14722347E-04	-0.14629364E-02	0.55054560E-01
-0.50000000E 00	0.16920269E-04	0.50768256E-04	-0.50601959E-02	0.52551299E-01
-0.70000000E 00	0.22862107E-04	0.12955070E-03	-0.12931824E-01	0.49638331E-01
-0.90000000E 00	0.17193146E-04	0.32666326E-03	-0.32649994E-01	0.46688318E-01
-0.98999999E 00	0.34561381E-05	0.68777800E-03	-0.68775177E-01	0.45673847E-01
-0.99900000E 00	0.48743095E-06	0.97438693E-03	-0.97436905E-01	0.44686913E-01

APPENDIX B: TABLE 2

A = .05, RHOP = 400, TAU = 1, DELTA = .01

LAMDA	J+(A) - J+(0)	J-(A) - J-(0)	CURR(A) - CURR(0)	PSIP(A) - PSIP(0)
0.99900000E 00	0.48719347E-02	0.24371839E-05	0.46282113E-02	0.17741036E-00
0.98999999E 00	0.34388900E-02	0.17280807E-04	0.17108023E-02	0.16814184E-00
0.90000000E 00	0.16333610E-02	0.85965730E-04	-0.69631338E-02	0.16512924E-00
0.70000000E 00	0.64781308E-03	0.11432171E-03	-0.10784388E-01	0.14076674E-00
0.50000000E 00	0.25385618E-03	0.84616244E-04	-0.82073212E-02	0.11532965E-00
0.30000000E-00	0.73581934E-04	0.39614737E-04	-0.38871765E-02	0.96541271E-01
0.10000000E-00	0.67055225E-05	0.54836273E-05	-0.54168701E-03	0.78149945E-01
-0.10000000E-00	0.54836273E-05	0.67055225E-05	-0.66471100E-03	0.61014920E-01
-0.30000000E-00	0.39614737E-04	0.73581934E-04	-0.73184967E-02	0.43030202E-01
-0.50000000E 00	0.84616244E-04	0.25385618E-03	-0.25302887E-01	0.24233937E-01
-0.70000000E 00	0.11432171E-03	0.64781308E-03	-0.64666748E-01	-0.42939186E-03
-0.90000000E 00	0.85965730E-04	0.16333610E-02	-0.16324997E-00	-0.25509655E-01
-0.98999999E 00	0.17280807E-04	0.34388900E-02	-0.34387207E-00	-0.32104492E-01
-0.99900000E 00	0.24371839E-05	0.48719347E-02	-0.48719025E-00	-0.43041587E-01

APPENDIX B: TABLE 3

A = .1, RHOP = 400, TAU = 1, DELTA = .01

LAMDA	J+(A) - J+(0)	J-(A) - J-(0)	CURR(A) - CURR(0)	PSIP(A) - PSIP(0)
0.99900000E 00	0.97438097E-02	0.48743386E-05	0.92563629E-02	0.29807627E-00
0.98999999E 00	0.68778098E-02	0.34561846E-04	0.34216195E-02	0.27911890E-00
0.90000000E 00	0.32667220E-02	0.17193239E-03	-0.13926506E-01	0.27443093E-00
0.70000000E 00	0.12956411E-02	0.22863969E-03	-0.21568298E-01	0.21998894E-00
0.50000000E 00	0.50768256E-03	0.16922504E-03	-0.16414642E-01	0.16211745E-00
0.30000000E-00	0.14716387E-03	0.79244375E-04	-0.77772141E-02	0.11941551E-00
0.10000000E-00	0.13396144E-04	0.10952353E-04	-0.10814667E-02	0.77521797E-01
-0.10000000E-00	0.10952353E-04	0.13396144E-04	-0.13284683E-02	0.38611360E-01
-0.30000000E-00	0.79244375E-04	0.14716387E-03	-0.14636993E-01	-0.22965819E-02
-0.50000000E 00	0.16922504E-03	0.50768256E-03	-0.50601959E-01	-0.45072943E-01
-0.70000000E 00	0.22863969E-03	0.12956411E-02	-0.12933540E-00	-0.10119885E-00
-0.90000000E 00	0.17193239E-03	0.32667220E-02	-0.32649994E-00	-0.15761381E-00
-0.98999999E 00	0.34561846E-04	0.68778098E-02	-0.68774605E 00	-0.17111206E-00
-0.99900000E 00	0.48743386E-05	0.97438097E-02	-0.97437477E 00	-0.19411242E-00

APPENDIX B: TABLE 4

A = .01, RHOP = 1600, TAU = 1, DELTA = .01

LAMDA	J+(A) - J+(0)	J-(A) - J-(0)	CURR(A) - CURR(0)	PSIP(A) - PSIP(0)
0.99900000E 00	0.38668513E-03	0.19343861E-06	0.36734343E-03	0.93300462E-01
0.98999999E 00	0.27292967E-03	0.13714889E-05	0.13577938E-03	0.89509249E-01
0.90000000E 00	0.12964010E-03	0.68228692E-05	-0.55277348E-03	0.88673890E-01
0.70000000E 00	0.51423907E-04	0.90748072E-05	-0.85592270E-03	0.80721319E-01
0.50000000E 00	0.20161271E-04	0.67204237E-05	-0.65183640E-03	0.72636247E-01
0.30000000E-00	0.58263540E-05	0.31366944E-05	-0.30803680E-03	0.67052126E-01
0.10000000E-00	0.53644180E-06	0.44703484E-06	-0.44822693E-04	0.61689645E-01
-0.10000000E-00	0.44703484E-06	0.53644180E-06	-0.53405762E-04	0.56767650E-01
-0.30000000E-00	0.31366944E-05	0.58263540E-05	-0.57792664E-03	0.51492453E-01
-0.50000000E 00	0.67204237E-05	0.20161271E-04	-0.20103455E-02	0.45988113E-01
-0.70000000E 00	0.90748072E-05	0.51423907E-04	-0.51345825E-02	0.38158715E-01
-0.90000000E 00	0.68228692E-05	0.12964010E-03	-0.12956619E-01	0.30475140E-01
-0.98999999E 00	0.13714889E-05	0.27292967E-03	-0.27290344E-01	0.29872417E-01
-0.99900000E 00	0.19343861E-06	0.38668513E-03	-0.38669586E-01	0.26480794E-01

APPENDIX B: TABLE 5

A = .05, RHOP = 1600, TAU = 1, DELTA = .01

LAMDA	J+(A) - J+(0)	J-(A) - J-(0)	CURR(A) - CURR(0)	PSIP(A) - PSIP(0)
0.99900000E 00	0.19334257E-02	0.96720760E-06	0.18367022E-02	0.36639225E-00
0.98999999E 00	0.13647377E-02	0.68580266E-05	0.67894161E-03	0.33937347E-00
0.90000000E 00	0.64821541E-03	0.34116209E-04	-0.27635098E-02	0.33250648E-00
0.70000000E 00	0.25708973E-03	0.45366585E-04	-0.42793751E-02	0.26545942E-00
0.50000000E 00	0.10074675E-03	0.33579767E-04	-0.32572746E-02	0.19569758E-00
0.30000000E-00	0.29191375E-04	0.15720725E-04	-0.15430450E-02	0.14584920E-00
0.10000000E-00	0.26524067E-05	0.21755695E-05	-0.21553040E-03	0.97665556E-01
-0.10000000E-00	0.21755695E-05	0.26524067E-05	-0.26321411E-03	0.53202637E-01
-0.30000000E-00	0.15720725E-04	0.29191375E-04	-0.29029846E-02	0.55858493E-02
-0.50000000E 00	0.33579767E-04	0.10074675E-03	-0.10042191E-01	-0.44041663E-01
-0.70000000E 00	0.45366585E-04	0.25708973E-03	-0.25665283E-01	-0.11252302E-00
-0.90000000E 00	0.34116209E-04	0.64821541E-03	-0.64786911E-01	-0.17930382E-00
-0.98999999E 00	0.68580266E-05	0.13647377E-02	-0.13646507E-00	-0.18771899E-00
-0.99900000E 00	0.96720760E-06	0.19334257E-02	-0.19334221E-00	-0.21431243E-00

APPENDIX B: TABLE 6

A = .1, RHOP = 1600, TAU = 1, DELTA = .01

LAMDA	J+(A) - J+(0)	J-(A) - J-(0)	CURR(A) - CURR(0)	PSIP(A) - PSIP(0)
0.99900000E 00	0.38668513E-02	0.19343861E-05	0.36734194E-02	0.65370059E 00
0.98999999E 00	0.27294159E-02	0.13715820E-04	0.13578385E-02	0.60872698E 00
0.90000000E 00	0.12964159E-02	0.68232417E-04	-0.55269003E-02	0.58872575E 00
0.70000000E 00	0.51419437E-03	0.90736896E-04	-0.85594654E-02	0.45745742E-00
0.50000000E 00	0.20147860E-03	0.67159533E-04	-0.65145493E-02	0.32081965E-00
0.30000000E-00	0.58397651E-04	0.31448901E-04	-0.30860901E-02	0.21776697E-00
0.10000000E-00	0.53197145E-05	0.43585896E-05	-0.43106079E-03	0.11751411E-00
-0.10000000E-00	0.43585896E-05	0.53197145E-05	-0.52738190E-03	0.23765922E-01
-0.30000000E-00	0.31448901E-04	0.58397651E-04	-0.58097839E-02	-0.75487912E-01
-0.50000000E 00	0.67159533E-04	0.20147860E-03	-0.20082474E-01	-0.17822322E-00
-0.70000000E 00	0.90736896E-04	0.51419437E-03	-0.51328659E-01	-0.31275749E-00
-0.90000000E 00	0.68232417E-04	0.12964159E-02	-0.12957191E-00	-0.44394410E-00
-0.98999999E 00	0.13715820E-04	0.27294159E-02	-0.27292824E-00	-0.46731532E-00
-0.99900000E 00	0.19343861E-05	0.38668513E-02	-0.38668442E-00	-0.51213777E 00

APPENDIX B: TABLE 7

A = .01, RHOP = 400, TAU = 10, DELTA = .01

LAMDA	J+(A) - J+(0)	J-(A) - J-(0)	CURR(A) - CURR(0)	PSIP(A) - PSIP(0)
0.99900000E 00	0.72700977E-02	0.66151551E-06	0.72039366E-02	0.74199677E-01
0.98999999E 00	0.53157806E-02	0.48768707E-05	0.48280954E-02	0.69650292E-01
0.90000000E 00	0.26777983E-02	0.26777387E-04	-0.	0.68861544E-01
0.70000000E 00	0.10906458E-02	0.40899962E-04	-0.29995441E-02	0.66197455E-01
0.50000000E 00	0.42462349E-03	0.35382807E-04	-0.31137466E-02	0.63166499E-01
0.30000000E-00	0.11801720E-03	0.20653009E-04	-0.19483566E-02	0.59585884E-01
0.10000000E-00	0.93579292E-05	0.42095780E-05	-0.41103363E-03	0.56292363E-01
		LAMDA IS ZERO		
-0.99999999E-02	0.67055225E-07	0.74505806E-07	-0.76293945E-05	0.54016341E-01
-0.30000000E-01	0.52899122E-06	0.78976154E-06	-0.78201294E-04	0.53650029E-01
-0.50000000E-01	0.12367964E-05	0.26077032E-05	-0.26035309E-03	0.53326055E-01
-0.69999999E-01	0.18775463E-05	0.66906214E-05	-0.66757202E-03	0.52976489E-01
-0.90000000E-01	0.16512349E-05	0.18000603E-04	-0.17976761E-02	0.52645452E-01
-0.98999999E-01	0.40233135E-06	0.44211745E-04	-0.44202805E-02	0.52546784E-01

APPENDIX B: TABLE 8

A = .05, RHOP = 400, TAU = 10, DELTA = .01

LAMDA	J+(A) - J+(0)	J-(A) - J-(0)	CURR(A) - CURR(0)	PSIP(A) - PSIP(0)
0.99900000E 00	0.36350608E-01	0.33076067E-05	0.36019921E-01	0.20567727E-00
0.98999999E 00	0.26578307E-01	0.24383771E-04	0.24139881E-01	0.16573310E-00
0.90000000E 00	0.13388753E-01	0.13388693E-03	-0.	0.17815858E-00
0.70000000E 00	0.54532290E-02	0.20449609E-03	-0.14996529E-01	0.16544986E-00
0.50000000E 00	0.21231771E-02	0.17692894E-03	-0.15570164E-01	0.14343557E-00
0.30000000E-00	0.59008598E-03	0.10326505E-03	-0.97379684E-02	0.11372314E-00
0.10000000E-00	0.46789646E-04	0.21055341E-04	-0.20589828E-02	0.86167898E-01
		LAMDA IS ZERO		
-0.99999999E-02	0.32037497E-06	0.37252903E-06	-0.37193298E-04	0.65812236E-01
-0.30000000E-01	0.26300550E-05	0.38743019E-05	-0.38528442E-03	0.62541194E-01
-0.50000000E-01	0.62063336E-05	0.13038516E-04	-0.12989044E-02	0.59721395E-01
-0.69999999E-01	0.93802810E-05	0.33438206E-04	-0.33340454E-02	0.56572936E-01
-0.90000000E-01	0.82580373E-05	0.90017915E-04	-0.89931488E-02	0.53439684E-01
-0.98999999E-01	0.20117732E-05	0.22108853E-03	-0.22106171E-01	0.52050725E-01

APPENDIX B: TABLE 9

A = .1, RHOP = 400, TAU = 10, DELTA = .01

LAMDA	J+(A) - J+(0)	J-(A) - J-(0)	CURR(A) - CURR(0)	PSIP(A) - PSIP(0)
0.99900000E 00	0.72701454E-01	0.66152425E-05	0.72039962E-01	0.36311102E-00
0.98999999E 00	0.53156495E-01	0.48767542E-04	0.48279762E-01	0.27990186E-00
0.90000000E 00	0.26777387E-01	0.26777387E-03	-0.	0.30950427E-00
0.70000000E 00	0.10906458E-01	0.40899217E-03	-0.29992819E-01	0.27997178E-00
0.50000000E 00	0.42464137E-02	0.35386533E-03	-0.31140327E-01	0.22981369E-00
0.30000000E-00	0.11801124E-02	0.20652264E-03	-0.19473076E-01	0.16388600E-00
0.10000000E-00	0.93549490E-04	0.42095780E-04	-0.41160583E-02	0.10194813E-00
		LAMDA IS ZERO		
-0.99999999E-02	0.65565109E-06	0.74505806E-06	-0.75340271E-04	0.57742119E-01
-0.30000000E-01	0.52601099E-05	0.77486038E-05	-0.76961517E-03	0.50477695E-01
-0.50000000E-01	0.12412667E-04	0.26077032E-04	-0.25959015E-02	0.44140868E-01
-0.69999999E-01	0.18760562E-04	0.66891313E-04	-0.66699982E-02	0.37191488E-01
-0.90000000E-01	0.16515143E-04	0.18002093E-03	-0.17984390E-01	0.30223988E-01
-0.98999999E-01	0.40235464E-05	0.44219196E-03	-0.44215202E-01	0.27068049E-01